ELSEVIER

Soil & Tillage Research 55 (2000) 1–29

Soil & Tillage Research

www.elsevier.com/locate/still

Invited Review

Field measurement of soil surface hydraulic properties by disc and ring infiltrometers A review and recent developments

Rafael Angulo-Jaramillo*, Jean-Pierre Vandervaere, Stéphanie Roulier, Jean-Louis Thony, Jean-Paul Gaudet, Michel Vauclin

Laboratoire d'étude des Transferts en Hydrologie et Environnement, LTHE UMR 5564 (CNRS, INPG, IRD, UJF), BP 53, 38041 Grenoble Cedex 9, France

Received 15 July 1999; received in revised form 8 November 1999; accepted 27 January 2000

Abstract

Soil management influences physical properties and mainly the soil hydraulic functions. Their measurement becomes one of the research preferences in this branch of applied soil science. Tension disc and pressure ring infiltrometers have become very popular devices for the in situ estimates of soil surface hydraulic properties. Their use for measuring solute–water transfer parameters of soils is now well established too. A number of publications testify that both devices have been extensively used all around the world for different purposes. In this review, a short introduction is devoted to the background theory and some examples are given to show how the theory can be used to determine hydraulic conductivity and sorptivity from measured cumulative infiltration. The methods of analysis of cumulative infiltration are based either on quasi-analytical solutions of the flow equation for homogeneous soil profile or on inverse parameter estimation techniques from the numerical solution of flow equation whether the soil profile is homogeneous or not. The disc infiltrometer has also been shown as a suitable device for inferring parameters describing the water-borne transport of chemicals through near saturated soils. Associated with conservative tracers, it has been recognized as a promising tool for the determination of both hydraulic and solute transport properties as well as for other parameters such as mobile/immobile water content fraction or exchange coefficient. An emphasis is put here on some published studies performed in different soils and environmental conditions focusing on heterogeneous soil profiles (crusted soils) or structured cultivated soils (aggregated soils), either when local water transport process is studied or when field spatial variability is investigated. Some new research studies such as water–solute transfer in structured or swelling–shrinking soils and multi-interactive solute transport are emerging. A number of challenges still remain unresolved for both theory and practice for tension and pressure infiltrometers. They include questions on how to consider and characterize saturated–unsaturated preferential flow or preferential transport process (including hydrodynamic instabilities) induced by biological activity (e.g. capillary macropores, earthworm holes or root channels) by specific pedagogical conditions (e.g. cracking, crusting) and by soil management practices (i.e. conservation tillage).

Keywords: Hydraulic conductivity; Sorptivity; Disc infiltrometer; Pressure infiltrometer; Field measurements

* Corresponding author. Tel.: +33-476-82-50-55; fax: +33-476-82-50-69.
E-mail address: angulo@hmg.inpg.fr (R. Angulo-Jaramillo)

0167-1987/00/$ – see front matter
PII: S0167-1987(00)00098-2

1. Introduction

In many applications dealing with environmental sciences, the knowledge of soil hydraulic properties is important: (i) to diagnose the hydrodynamic functioning of soils in relation to the natural and/or anthropogenic constraints which are applied, and (ii) to simulate the physical processes in order to establish a prognosis on the order of magnitude of the hydraulic fluxes able, for instance, to make water and nutrients available for the plant rooting system, or to advect chemicals leading to point or diffuse pollution of the groundwater table. Physically based modeling of coupled water and solute transport requires the knowledge of soil properties that have to be estimated with sufficient precision. On this way, the development of in situ techniques to determine both the saturated and unsaturated hydraulic properties of the soil surface has received increasing attention in the recent years, in particular to assess the role of preferential flow pathways in the soil management practices. Estimation of field soil properties represents then a challenge for soil scientists.

Infiltration-based methods are recognized as valuable tools to investigate hydraulic and transport soil properties. In particular, two complementary methods appear to be interesting in the study of saturated and near saturated soil behavior. They are the confined one-dimensional pressure ring-infiltrometer and the unconfined three-dimensional tension disc infiltrometer methods. In addition to some theoretical developments, the operative assumptions are briefly summarized for both steady-state and transient flow infiltration conditions.

Compilation of some relevant results obtained with such experimental devices are reviewed and discussed here. They include estimates of sorptivity, hydraulic conductivity and their relations with the capillary pressure for either different homogeneous and layered or heterogeneous soils under a variety of climatic and soil use conditions. Also, some other soil properties are presented, such as mean characteristic pore size and fraction of mobile–immobile soil water content, which allow the study of transport processes. The limitations of these techniques are briefly discussed and some further developments are suggested.

2. Basic design and operation

2.1. Tension disc infiltrometers

The home made system called TRIMS (triple ring infiltrometers at multiple suction) consists of three sets (Fig. 1) constructed out of Plexiglas following the design of Perroux and White (1988). The base of each

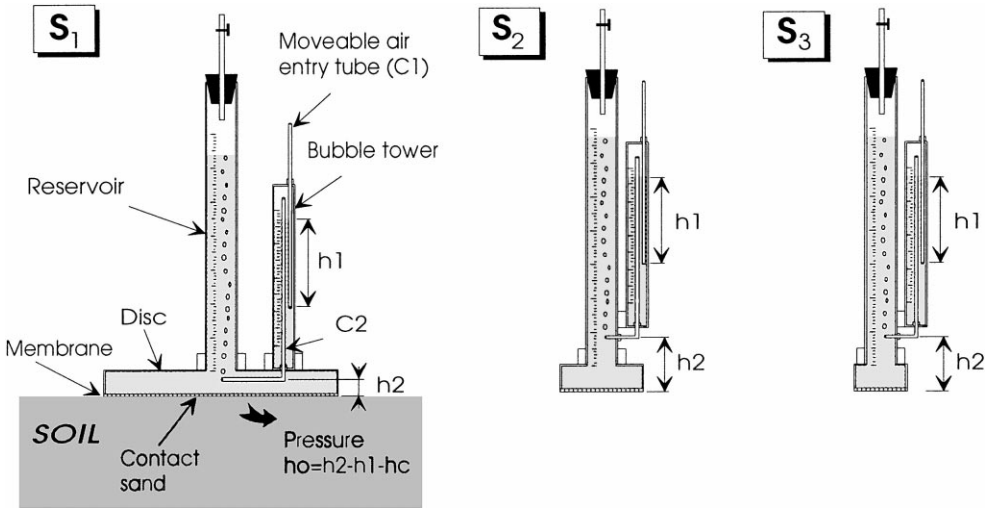

Fig. 1. Disc infiltrometers S1, S2 and S3 of diameters 250, 80 and 48.5 mm, respectively.

disc of diameter 250 mm (S1), 80 mm (S2), and 48.5 mm (S3) is covered by a nylon cloth of 20 μm mesh. A graduated reservoir tower provides the water supply, and a bubble tower with a moveable air-entry tube (C1) imposes the pressure head h_o of the water at the cloth base. The pressure head h_o is the difference of heights $h_2-h_1-h_c$, where h_2 is constant and represents the height of air-supply tube (C2) from the base of the disc (Fig. 1), h_1 is adjustable and represents the difference between the bottom of air tube (C1) and the water level in the bubble tower which is kept constant, and h_c represents a correction term due to capillary effect in the system. If $h_2<h_1+h_c$, then the applied pressure h_o is negative (i.e. h_o below the atmospheric pressure).

For measurements under tension, it is essential that intimate hydraulic contact be maintained between the soil surface and the source of water. This is generally achieved by pouring at the surface a layer of sand which should be made as thin as possible and ready to accept emplacement of the disc infiltrometer which has already been set at h_o. Immediately after placement, excess contact sand outside the rim of the infiltrometer has to be swept away to avoid any horizontal wicks of sand lying across the soil surface. For every imposed value h_o, the cumulative infiltration, $I(t)$, is recorded either by noting the water level drop in the reservoir tower (Fig. 1) or by using a pressure transducer (i.e. Ankeny et al., 1988). More details can be found in Vauclin and Chopart (1992).

2.2. Pressure ring infiltrometer

Typical pressure single-ring infiltrometer is illustrated in Fig. 2. Water is supplied to the soil surface at a positive pressure head h_o through a sealed top lid either by a Mariotte bottle with a moveable air tube allowing a wide range of h_o (Fig. 2a) similar to the Guelph Permeameter reservoir (Reynolds et al., 1985; Reynolds and Elrick, 1990; Vauclin et al., 1994), or by a small capillary tube also acting as a measuring burette (Fig. 2b). This tube can be positioned either horizontally to infiltrate water at a constant head, or vertically to infiltrate water at a continuous falling

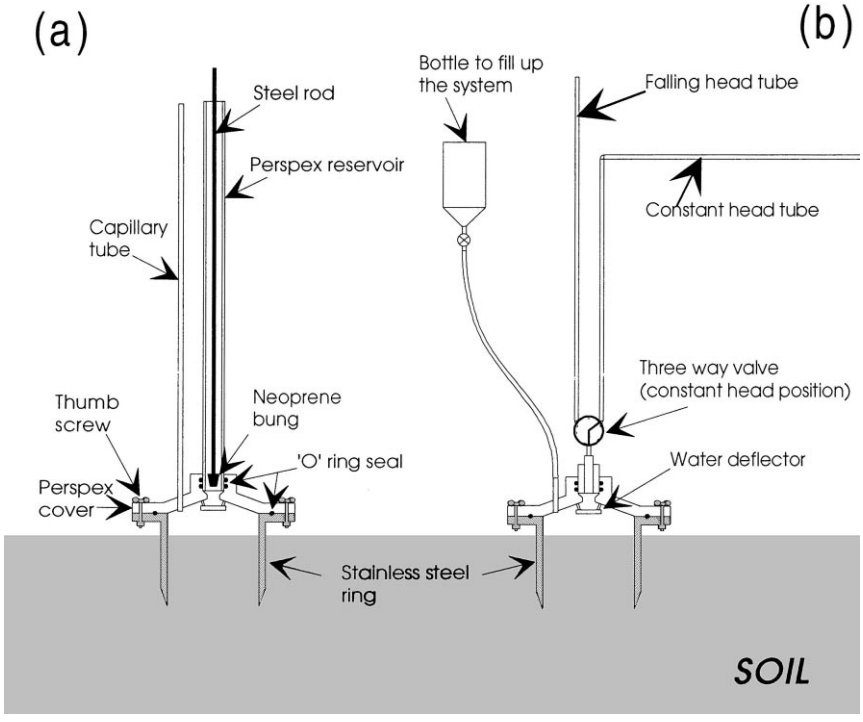

Fig. 2. Schema of the pressure ring infiltrometer (98 mm in diameter) for constant head (a), and both constant head and falling head (b).

head. Because of the positive heads used in the tests, up thrust of the sealing lid of the device may occur. The ring therefore has to be weighed down to prevent the hydraulic force lifting the ring out of the soil. The ring used in the tests reported here has a diameter of 98 mm and can be driven into the soil to a maximum depth of 60 mm. More details dealing with the operational aspects are given in Vauclin et al. (1994), Elrick et al. (1995) and Youngs et al. (1995) for configuration (2a) and in Fallow et al. (1994) and Gérard-Marchant et al. (1997) for configuration (2b). It should be noted that constant head–falling-head ring infiltrometer (Fig. 2b) is particularly appropriate for slowly permeable soils, landfill lining and capping porous materials.

3. Description of water flow from tension disc infiltrometers

The following axisymmetric form of Richard's equation can be used to describe the flow of water from a disc (Warrick, 1992):

$$C(h)\frac{\partial h}{\partial t} = \frac{\partial}{\partial z}\left[K(h)\left(\frac{\partial h}{\partial z} - 1\right)\right] + \frac{\partial}{\partial r}\left[K(h)\frac{\partial h}{\partial r}\right] + \frac{K(h)}{r}\frac{\partial h}{\partial r} \quad (1)$$

where $C(h)=\mathrm{d}\theta/\mathrm{d}h$ is the soil water capillary capacity function [L^{-1}], θ being the volumetric water content [L^3L^{-3}], h the water pressure head [L], $K(h)$ the hydraulic conductivity function [LT^{-1}], r and z are radial and vertical coordinates [L], respectively. Note that Eq. (1) assumes that the soil is isotropic, although not necessarily homogeneous.

Assuming initial uniform soil water, pressure pattern leads to

$$h(r,z,t) = h_\mathrm{n}, \quad z \geq 0, \ \ r \geq 0, \ \ t < 0 \quad (2)$$

Infiltration from a tension disc infiltrometer maintained at water pressure h_o corresponds to the following boundary conditions:

$$h(r,0,t) = h_\mathrm{o}, \quad z = 0, \ \ r \leq r_\mathrm{d}, \ \ t \geq 0 \quad (3)$$

where r_d is the disc radius.

Beyond the rim of the disc no vertical flow is assumed or imposed:

$$\left(\frac{\partial h}{\partial z} - 1\right) = 0, \quad z = 0, \ \ r > r_\mathrm{d}, \ \ t \geq 0 \quad (4)$$

Subsurface boundary conditions are assumed to be located far enough from the supply source so that they do not affect the infiltration process.

Various techniques have been developed to infer hydraulic properties from measurements of either transient flow rates, q_o [LT^{-1}], or steady ones, $q_{\mathrm{o}\infty}$, that emanate from a disc set at the water pressure head h_o. Methods are based either on quasi-analytical solutions of the flow equation for homogeneous soil profile, or numerical solutions of Eq. (1) through inverse parameter estimation techniques whether the soil profile is homogeneous or not.

3.1. Steady-state flow

The steady-state flow theory and its applications have been presented and discussed elsewhere (Perroux and White, 1988; Smettem and Clothier, 1989; White and Perroux, 1989; Clothier and Smettem, 1990; Thony et al., 1991; Warrick, 1992; White et al., 1992; Quadri et al., 1994; and many others). Let us summarize here the main salient features.

Wooding's (1968) equation which is at the heart of most of these analyses approximates the steady infiltration rate, $q_{\mathrm{o}\infty}$, from a disc as

$$q_{\mathrm{o}\infty} = K_\mathrm{o} + \frac{4\phi_\mathrm{o}}{\pi}\frac{1}{r_\mathrm{d}} \quad (5)$$

where ϕ_o is the matrix flux potential defined by

$$\phi_\mathrm{o} = \int_{\theta_\mathrm{n}}^{\theta_\mathrm{o}} D(u)\,\mathrm{d}u = \int_{h_\mathrm{n}}^{h_\mathrm{o}} K(u)\,\mathrm{d}u, \quad \theta_\mathrm{o} \geq \theta_\mathrm{n}, \ \ h_\mathrm{n} \leq h_\mathrm{o} \quad (6)$$

In these equations, K_o is the hydraulic conductivity at the imposed pressure head h_o, $K_\mathrm{o}=K(h_\mathrm{o})$, $D(\theta)$ is the capillary diffusivity [L^2T^{-1}]. The subscript o refers to the condition imposed at the supply surface of the disc, and the subscript n denotes the antecedent condition prevailing in the soil before the infiltration takes place. The flow is then controlled by two soil properties: the hydraulic conductivity K_o which accounts for the effect of gravity and that of the sorptivity $S_\mathrm{o}=S(h_\mathrm{o})$ which represents, in an integral sense, the soil's capillarity. Eq. (5) can be solved for K_o and ϕ_o by using either multiple radii (at the same value h_o) or multiple head (for a given disc radius) procedures.

3.1.1. Multiple disc approach

From measurement of steady-state infiltration fluxes, $q_{o\infty}$, emanating from two discs of contrasting radius, r_1 and r_2, namely q_1 and q_2, the simultaneous solution of Eq. (5) gives (Smettem and Clothier, 1989; Thony et al., 1991):

$$K_o = \frac{q_1 r_1 - q_2 r_2}{r_1 - r_2} \tag{7a}$$

and

$$\phi_o = \frac{\pi}{4} \frac{q_1 - q_2}{1/r_1 - 1/r_2} \tag{7b}$$

If q_1 and q_2 are derived from, respectively, n_1 and n_2 replications of steady flow measurements, and if K_o and ϕ_o are assumed to be normally distributed over a field, then their standard errors are (Scotter et al., 1982):

$$s_{K_o} = \frac{[(s_1 r_1)^2/n_1 + (s_2 r_2)^2/n_2]^{1/2}}{r_1 - r_2} \tag{8a}$$

$$s_{\phi_o} = \frac{\pi}{4} \frac{[s_1{}^2/n_1 + s_2{}^2/n_2]^{1/2}}{1/r_1 - 1/r_2} \tag{8b}$$

where s_1 and s_2 are the standard deviations of q_1 and q_2, respectively.

Examples of applications can be found in Thony et al. (1991), Vauclin and Chopart (1992) with n_1 and n_2 varying from 3 to 5 for r_1=125 mm and r_2=40 mm.

An alternative approach consists in using three discs of different radii (Thony et al., 1991) and to perform a linear regression between measured values of q_i and $1/r_i$ (Eq. (5)), thus providing the intercept K_o, and the slope $4\phi_o/\pi$ which straightforwardly gives ϕ_o. The statistical analysis makes also possible the estimates of the uncertainties associated with K_o and ϕ_o values thus obtained.

If an exponential soil water diffusivity, $D(\theta)$, scaled by sorptivity S_o at h_o is assumed (Reichardt et al., 1972; Brutsaert, 1979; White, 1987), it is possible to show that

$$\phi_o = \frac{b S_o{}^2}{\theta_o - \theta_n} \tag{9}$$

where the envelope of the possible values of b is delimited by the Dirac delta soil (b=0.5) and the linear soil ($b=\frac{1}{4}\pi$). It is frequently assumed that $b\approx$0.55 for a field soil (White and Sully, 1987). Then having measured ($\theta_o-\theta_n$), it is possible to deduce S_o from Eq. (9), ϕ_o being obtained by solving Eq. (5). Final water content, θ_o, is the mean value of measurements made underneath each disc.

3.1.2. Multiple head approach

Ankeny et al. (1991) started with Eq. (5) and measured infiltration rates at two pressure heads h_1 and h_2 successively applied to the same disc. This leads to two equations and four unknowns:

$$q_1 = K_1 + \frac{4}{\pi r_d}\phi_1 \tag{10a}$$

$$q_2 = K_2 + \frac{4}{\pi r_d}\phi_2 \tag{10b}$$

where K_1=$K(h_1)$, K_2=$K(h_2)$, ϕ_1=$\phi(h_1)$ and ϕ_2=$\phi(h_2)$. By assuming a constant ratio A=$K(h)/\phi(h)$ throughout the pressure range h_1 to h_2 (Philip, 1985, 1986) and deriving an approximate expression for the difference ($\phi_1-\phi_2$), Ankeny et al. (1991) obtained three equations with three unknowns which are simultaneously solved for the two conductivities K_1 and K_2, from which ϕ_1 and ϕ_2 may also be calculated. Applying this procedure to sequential pairs of measurements produces a piecewise $K(h)$ curve.

It should be noted that considering an exponential relationship between K and h (Gardner, 1958):

$$K(h) = K_{fs}\, e^{\alpha h} \tag{11}$$

where K_{fs} is the apparent field-saturated hydraulic conductivity, and α is a constant, leads to the following exact expression for ($\phi_1-\phi_2$):

$$\phi_1 - \phi_2 = \frac{K_1 - K_2}{\alpha} = \frac{(h_1 - h_2)(K_1 - K_2)}{\ln(K_1/K_2)} \tag{12}$$

Rather than fitting infiltrometer measurements by a piecewise relationship made at sequential head pressures, Logsdon and Jaynes (1993) developed a nonlinear regression technique for fitting simultaneously all the data. Introducing Eq. (11) into Eq. (6) transforms Eq. (5) into

$$q_{o\infty} = \left[1 + \frac{4}{\alpha\pi r_d}\right] K_{fs}\, e^{\alpha h_o} \tag{13}$$

which was iteratively solved for α and K_{fs}. The number of measurements (h_o, $q_{o\infty}$) has to be greater than 2

to avoid spurious regressions.Wooding's solution, Eq. (5), was extended to the case of small radii by Weir (1987). In such cases, small radii correspond to large capillary effects relative to the gravity ones. Weir's analytical approximation considers a dimensionless radius ($\frac{1}{2}\alpha r_d$) that depends on the soil parameter α (Eq. (11)). It has been shown that the Weir approximation is more accurate than Wooding's for dimensionless radius less than 0.4.

3.2. Transient flow

Although the methods of analysis based on the Wooding's steady flow equation (5) have been widely used and compared over the last decade (e.g. Hussen and Warrick, 1993; Logsdon and Jaynes, 1993; Cook and Broeren, 1994), several researchers oriented their work on finding analytical solutions for transient flow from disc infiltrometers. Turner and Parlange (1974), Warrick and Lomen (1976), Warrick (1992), Haverkamp et al. (1994), Smettem et al. (1994) and Zhang (1997) proposed different approaches to account for the circular geometry of the source. Restrictions in the use of Wooding's equation, uncertainties about the time at which steady infiltration flux is attained, together with the fact that much useful information is lost by ignoring the transient stage (Logsdon, 1997) have strengthened the need for a transient three-directional infiltration equation for disc infiltrometers. Analysis of transient flow means shorter experiments and smaller sampled volumes of soil which is obviously in better agreement with assumptions of homogeneity and initial water content uniformity. The most recent expressions (Warrick, 1992; Haverkamp et al., 1994; Zhang, 1997) have in common the following two-term form of the cumulative infiltration equation:

$$I(t) = C_1\sqrt{t} + C_2 t \tag{14}$$

but they differ by the expressions of the coefficients C_1 and C_2. The validity of Eq. (14) was discussed in Vandervaere et al. (2000a). Warrick (1992) proposed expressions of C_1 and C_2 for small times by assuming a constant diffusivity. Zhang (1997) gave empirical values for C_1 and C_2. Haverkamp et al. (1994), using previous works by Turner and Parlange (1974) and Smettem et al. (1994), proposed the following physically based expressions valid for times not approaching steady-state:

$$C_1 = S_o \tag{15}$$

$$C_2 = K_n + \tfrac{1}{3}(2-\beta)(K_o - K_n) + \frac{\gamma}{r_d(\theta_o - \theta_n)} S_o{}^2 \tag{16}$$

where β is a parameter depending on the capillary diffusivity function. It lies in the interval [0, 1], and γ is a constant approximately equal to 0.75.

Except for rare occasions, where the soil is initially at a high moisture content, the condition $K_n \ll K_o$ is fulfilled. Then, if an average value of 0.6 is taken for β, Eq. (14) simply reduces to

$$I(t) = S_o\sqrt{t} + \tfrac{7}{15}K_o t + \frac{0.75}{r_d(\theta_o - \theta_n)} S_o{}^2 t \tag{17}$$

The first term of the right-hand side of Eq. (17) corresponds to the vertical capillary flow and dominates the infiltration during its early stage. The second term corresponds to the gravity-driven vertical flow and the third one represents the lateral capillary flow component. One important feature of Eq. (17) is the fact that the difference between axisymmetric and one-dimensional vertical infiltration ($r_d \to \infty$), i.e. the water moving laterally by capillary, is linear with time. This was apparently ignored by Zhang (1997) who assumed coefficient C_2 to depend only on K_o and not on S_o. Eq. (17) appears as a three-dimensional extension of the well-known one-dimensional Philip (1957b) infiltration equation:

$$I(t) = S_o\sqrt{t} + At \tag{18}$$

The relative weights of the three terms of Eq. (17) play a decisive role in quantifying the accuracy with which S_o and K_o can be estimated (Vandervaere et al., 2000b). For example, if the second term of the right-hand side of Eq. (17) is negligible as compared to the third one, this means that the infiltration process is controlled only by capillarity and an accurate estimation of K_o is unlikely. Note that this kind of limitation is not only inherent to transient flow analysis but also affects the accuracy of methods based on steady-state flow analysis. Different methods to infer S_o and K_o values from C_1 and C_2 are described in Vandervaere et al. (2000b) depending on whether use is made of either one or several disc radii and either one or several h_o values.

One method of analysis presented in White and Sully (1987) makes use of both transient and steady-

state flow regime. It consists in assuming that S_o can be estimated by neglecting both gravity and lateral diffusion effects at the beginning of the axisymmetric infiltration process. Cumulative infiltration is then approximated by Philip's (1957a) equation established for one-dimensional horizontal infiltration:

$$I(t) = S_0 t^{1/2} \tag{19}$$

Note that Eq. (19) is equivalent to Eq. (17), where the two terms linear with time are omitted. Then, S_o can be determined as the slope of I vs. $\sqrt{t}$ during a time interval T, as small as possible, over which Eq. (19) is considered valid:

$$S_0 = \overline{\left[\frac{dI}{d(\sqrt{t})}\right]_T} \tag{20}$$

However, Eq. (20) must be carefully considered for at least two reasons.

1. In the case of soils with important gravity flow effects (i.e. sands), the term $S_o\sqrt{t}$ can rapidly be dominated by the K_o term in Eq. (17); on the other hand, in the case of soils exhibiting large capillary effects (i.e. clays), the term $S_o\sqrt{t}$ can rapidly be dominated by the S_o^2 lateral term in Eq. (17). Thus, it is not sure that any experimental condition exists at all, where Eq. (20) can be used with reasonable confidence and precision. As a matter of fact, the chosen time interval T is likely to strongly influence the calculated S_o values (Bonnell and Williams, 1986).
2. Tension disc infiltrometers are usually placed on a layer of sand to ensure hydraulic contact between the infiltrometer and the soil. The sand is normally chosen for its high conductivity so that no impeding effect modifies the steady-state infiltration flux. However, the effects of this layer on the first stages of infiltration can be important enough to mask the portion of the infiltration curve desired for analysis (Vandervaere et al., 1997, 2000a).

An alternative to the use of Eq. (20) is (White et al., 1992):

$$S_0 = \lim_{t\to 0}\left\{\frac{dI}{d(\sqrt{t})}\right\} \tag{21}$$

The solution of Eq. (21) is guaranteed if Eq. (14) is used with the following transformation (Vandervaere et al., 1997, 2000a):

$$\frac{dI}{d(\sqrt{t})} = C_1 + 2C_2\sqrt{t} \tag{22}$$

which also allows C_2 to be determined.

After S_o has been estimated, hydraulic conductivity is calculated by subtraction, using either steady flow through Eqs. (5) and (9):

$$K_o = q_{o\infty}\frac{4b}{\pi r_d(\theta_o - \theta_n)}S_o^2 \tag{23}$$

or transient flow by combining Eqs. (5), (15) and (16):

$$K_o = \frac{3}{2-\beta}\left[C_2 - \frac{\gamma S_o^2}{r_d(\theta_o - \theta_n)}\right] \tag{24}$$

Eqs. (23) and (24) can provide accurate estimates of K_o only if K_o is not too small as compared to $q_{o\infty}$ and C_2. This condition must be verified a posteriori.

3.3. Inverse method

An alternative to direct estimates of soil hydraulic properties is the use of inverse methods when in situ conditions differ strongly from assumptions required for the use of semi-analytical solutions of the flow equation. This is the case of heterogeneous soil profiles, i.e. non-uniform water content distribution, multi-layered system. The inverse procedure combines the Levenberg–Marquardt (Marquardt, 1963) non-linear parameter optimization method with a numerical solution of the axisymmetric unsaturated flow equation (Eq. (1)). Simunek and van Genuchten (1996, 1997), Simunek et al. (1998) recently suggested a numerical method to estimate hydraulic properties from cumulative infiltration data from a disc infiltrometer at several consecutive pressure heads. Data required for a successful inversion, in addition to the cumulative infiltration evolution with time, include measurements of initial and final water contents. Using numerical simulated data, they showed that the method can provide information not only on the hydraulic conductivity function as it is usually the case when invoking quasi-analytical methods, but also on the soil water retention curve.

The objective function to be minimized during the parameter estimation process can be formulated using either cumulative infiltration data only, or cumulative infiltration data in combination with additional infor-

mation such as the observed water content corresponding to the initial supply pressure head or transient pressure head, and/or water content measurements within the soil profile. The objective function for multiple measurement sets is defined as (Simunek and van Genuchten, 1996):

$$\mathrm{OF}(\mathbf{b}, q_1, \ldots, q_m) = \sum_{j=1}^{m} \left(v_j \sum_{j=1}^{n_j} w_{ij} [q_j^*(t_i) - q_j(t_i, \mathbf{b})]^2 \right) \tag{25}$$

where m represents the different sets of measurements (such as the cumulative infiltration data, or additional information), n_j the number of measurements in a particular set, $q_j^*(t_i)$ are the specific measurements at time t_i for the jth measurement set, $\mathbf{b}$ the vector of optimized parameters, $q_j(t_i, \mathbf{b})$ are the corresponding model predictions for the parameter vector $\mathbf{b}$, and v_j and $w_{i,j}$ are weights associated with a particular measurement set or point, respectively. The coefficients v_j, which minimize differences in weighting between different data types because of different absolute values and numbers of data involved, is given by (Clausnitzer and Hopmans, 1995; Clausnitzer et al., 1998; Simunek et al., 1998)

$$v_j = \frac{1}{n_j \sigma_j^2} \tag{26}$$

This defines the objective function as an average weighted squared deviation normalized by measurement variances σ_j^2.

4. Description of flow from ring infiltrometers

Basically the flow from a ring infiltrometer set at a positive pressure head H is controlled by the saturated hydraulic conductivity K_{fs} which accounts for the gravity effect and by the matrix flux potential ϕ_{m} which represents the capillary effect. From Eq. (6), ϕ_{m} is defined as

$$\phi_{\mathrm{m}} = \int_{h_{\mathrm{n}}}^{0} K(u)\, \mathrm{d}u \tag{27}$$

As for tension disc infiltrometer, various techniques based on either transient or steady-state water flow approaches have been used to infer soil hydraulic properties from ponded ring infiltration tests.

4.1. Steady-state flow

It is possible to show (Reynolds and Elrick, 1990; Elrick and Reynolds, 1992b) that the steady-state flow rate out of a ring infiltrometer is given by

$$q_{\mathrm{o}\infty} = K_{\mathrm{fs}} \left(1 + \frac{H}{\pi r_{\mathrm{d}} G} \right) + \frac{\phi_{\mathrm{m}}}{\pi r_{\mathrm{d}} G} \tag{28}$$

where

$$G = 0.316 \frac{d}{r_{\mathrm{d}}} + 0.184 \tag{29}$$

is a shape parameter, and d is the depth of insertion of the ring into the soil (Fig. 2).

The first term of the right-hand side of Eq. (28) represents the gravitational effect, the second one corresponds to the influence of the ponded head, H, and the third term represents the contribution of the capillarity to the soil water flow.

Applying successively to the same ring, two positive hydraulic heads H_1 and H_2 allows to solve simultaneously the resulting two equations (28) for K_{fs} and ϕ_{m}, from which it is also possible to calculate the parameter α of Eq. (11) as

$$\alpha = \frac{K_{\mathrm{fs}}}{\phi_{\mathrm{m}}} \tag{30}$$

4.2. Transient flow

The early-time transient flow of water from pressure infiltrometer with ponded head takes the form

$$I = S_H t^{1/2} \tag{31}$$

where S_H may be thought of as a ''ponded'' sorptivity. It incorporates the effects of both hydrostatic pressure in the ring and unsaturated soil capillarity. It may be expressed as (White and Sully, 1987):

$$S_H = \left[2(\theta_{\mathrm{o}} - \theta_{\mathrm{n}}) K_{\mathrm{fs}} H + \frac{\phi_{\mathrm{m}}}{b} \right]^{1/2} \tag{32}$$

It should be reminded that the validity of Eq. (31) relies on the premise that the infiltration is not significantly affected by gravity, that it is especially the case for slowly permeable soils such as clay liners. Fallow et al. (1994), Elrick et al. (1995) have presented results obtained by constant and falling head conditions applied to a ring infiltrometer (Fig. 2).

Recently Gérard-Marchant et al. (1997) have extended the approach initially developed for rigid soils to swelling materials.

Estimation of hydraulic parameters is obtained by fitting the infiltration equation on the experimental measured $I(t)$ data (e.g. by the single or double-ring infiltrometer methods). The goodness of fit is used as a criterion to justify the choice of the infiltration equation. For example, six different infiltration equations in addition to Eq. (18) were analyzed by Haverkamp et al. (1988) in terms of precision, choice of parameters with particular emphasis on their time-dependence, and applicability for predictive use. Three and four parameter-equations were developed and were found to be more useful than two parameter-equations. Estimated parameter confidence intervals using simulated infiltration data were also studied by Clausnitzer et al. (1998). Their results have shown that extending the duration of data acquisition leads to estimate parameters with higher degree of confidence to a more precise estimate of that confidence, and to a better defined minima in the objective function.

5. Some characteristic time and length scales

Water-source geometry, capillarity and gravity driving forces combine to dictate the pattern of water flux entering the soil during multidimensional infiltration. Two characteristic time scales and associated lengths are classically used to describe such a water flow.

The first one (Philip, 1969), related to gravity

$$t_{\mathrm{grav}} = \left(\frac{S_{\mathrm{o}}}{K_{\mathrm{o}}}\right)^2 \tag{33}$$

indicates the time after which gravity dominates one-dimensional vertical infiltration. The associated capillary length scale (White and Sully, 1987; Warrick and Broadbridge, 1992) is defined as

$$\lambda_{\mathrm{c}} = (K_{\mathrm{o}} - K_{\mathrm{n}})^{-1} \int_{h_{\mathrm{n}}}^{h_{\mathrm{o}}} K(h)\,\mathrm{d}h = \frac{\phi_{\mathrm{o}}}{K_{\mathrm{o}}} \tag{34}$$

Substituting Eqs. (6) and (9) into Eq. (34), and assuming that $K_{\mathrm{n}} \ll K_{\mathrm{o}}$ (soils at field capacity or dryer) leads to

$$\lambda_{\mathrm{c}} = \frac{bS_{\mathrm{o}}^2}{(\theta_{\mathrm{o}} - \theta_{\mathrm{n}})K_{\mathrm{o}}} \tag{35}$$

Eq. (35) shows that λ_{c} is a macroscopic length scale that represents the relative magnitude of the capillary and gravity forces which prevail during the infiltration process from a source maintained at θ_{o} into a soil initially at θ_{n}. Additionally, when an exponential relationship $K(h)$ (Eq. (11)) is considered, it follows from Eq. (34) that

$$\lambda_{\mathrm{c}} = \frac{1}{\alpha} \tag{36}$$

Typical values of α can be found in Elrick and Reynolds (1992b). They range from 1 for compacted structures, i.e. clay materials, to 36 for coarse and gravelly sands as well as for structured soils.

From Laplace capillary theory, a characteristic mean pore radius λ_{m} may be defined as

$$\lambda_{\mathrm{m}} = \frac{\sigma}{\rho_{\mathrm{w}} g}\frac{1}{\lambda_{\mathrm{c}}} = \frac{\sigma}{\rho_{\mathrm{w}} g}\frac{(\theta_{\mathrm{o}} - \theta_{\mathrm{n}})K_{\mathrm{o}}}{bS_{\mathrm{o}}^2} \tag{37}$$

where σ is the surface tension (73 mN/m), ρ_{w} the density of water and g is the acceleration due to gravity. This length scale defines mean characteristic pore sizes that are hydraulically functioning at the imposed water pressure head h_{o}.

The second characteristic time scale is related to the impact of the geometry of the water source. For circular surfaces, Philip (1969) considered the time t_{geom} after which the geometric effect dominates the capillary forces of the soil in drawing water from the source. It is defined as

$$t_{\mathrm{geom}} = \left(\frac{r_{\mathrm{d}}(\theta_{\mathrm{o}} - \theta_{\mathrm{n}})}{S_{\mathrm{o}}}\right)^2 \tag{38}$$

Thus, from measurements of sorptivity and hydraulic conductivity at different negative and positive water pressure head along with the value of $(\theta_{\mathrm{o}} - \theta_{\mathrm{n}})$ it is possible to deduce the relative roles played by capillarity, gravity and geometry on water flow and to infer pore sizes hydraulically functioning at different values of pressure head.

In Section 7 hereafter, results obtained in different situations by these various approaches will be presented and briefly discussed.

6. Description of water and solute flow from a tension disc infiltrometer

Two phenomena among others have led to reassess the description and modeling of solute transport in

unsaturated soils: (i) deeper penetration of surface-applied chemicals in the field than it can be expected by classical convection–dispersion approach; (ii) laboratory soil column observations of asymmetry and tailing of breakthrough curves in the case of non-adsorption solutes. To account for these phenomena, it is assumed that there are two distinct soil water regions in the system (Coats and Smith, 1964; van Genuchten and Wierenga, 1976; Gaudet et al., 1977): one region designated as the mobile water region, where solute transport takes place by convection and diffusion, and another one, termed as immobile region, where solute transfer occurs by diffusion only. Then the total volumetric water content is

$$\theta = \theta_{\mathrm{m}} + \theta_{\mathrm{im}} \tag{39}$$

where subscripts m and im refers to the mobile and immobile fractions, respectively.

The corresponding one-dimensional two region mobile–immobile water model under steady-state water flow may be written as

$$\theta_{\mathrm{m}} \frac{\partial C_{\mathrm{m}}}{\partial t} + \theta_{\mathrm{im}} \frac{\partial C_{\mathrm{im}}}{\partial t} = \theta_{\mathrm{m}} D_{\mathrm{m}} \frac{\partial^2 C_{\mathrm{m}}}{\partial z^2} - q_{\infty 1\mathrm{D}} \frac{\partial C_{\mathrm{m}}}{\partial z} \tag{40}$$

where solute concentrations in the mobile and immobile phases are denoted as C_{m} and C_{im}, respectively, and D_{m} is the dispersion coefficient in the mobile phase [$\mathrm{L^2T^{-1}}$].

Solute exchange between the mobile and immobile regions is described by

$$\theta_{\mathrm{im}} \frac{\partial C_{\mathrm{im}}}{\partial t} = \alpha^* (C_{\mathrm{m}} - C_{\mathrm{im}}) \tag{41}$$

where α^* [$\mathrm{T^{-1}}$] is the mass-transfer rate parameter for exchange between the two phases. The total solute concentration, C^*, in the soil is given by

$$\theta C^* = \theta_{\mathrm{m}} C_{\mathrm{m}} + \theta_{\mathrm{im}} C_{\mathrm{im}} \tag{42}$$

During last years, disc infiltrometers have been proposed as a means to infer some of the parameters describing the water-borne transport of chemicals through soils near saturation. Clothier et al. (1992) described a method where a tension infiltrometer and conservative tracer (bromide) were used to measure the mobile soil water content, θ_{m}. Once the steady-state regime of infiltration $q_{\mathrm{o}\infty}$ (Eq. (5)) was reached, the disc was removed for refilling with a tracer solution at concentration C_{o}. The disc was then immediately replaced at the same location. After penetration of the solution to a specified depth, soil cores were rapidly taken underneath the disc (Fig. 3). Considering that at the time of sampling, the immobile region remained free of tracer, and that the solute concentration in the mobile phase reached the imposed concentration C_{o} (which would be equivalent to consider α^* to be negligible at the sampling time), the mass conservation equation (42) reduces to

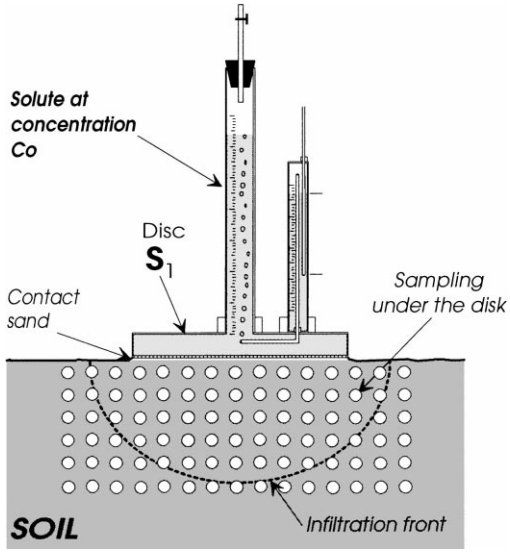

Fig. 3. Schematic representation of the experimental set up for water and solute disc infiltration.

$$\theta_{\mathrm{m}} = \theta \frac{C^*}{C_{\mathrm{o}}} \tag{43}$$

where both C^* and θ can be measured from soil samples, and C_{o} is the known solute concentration imposed by the disc.

Clothier et al. (1995) extended their single-tracer methodology for the estimation of α^*. After having removed the disc and taken samples for θ_{m} estimates (Eq. (43)), the infiltration zone has been covered with a plastic sheet to prevent evaporation and to allow redistribution of soil solution. Two and 14 days later, new cores were extracted from adjacent sectors within the area where the disc had originally been set up. The corresponding theoretical sampling variance of C^* at different times is expressed as

$$\sigma^2_{C^*}(t) = \frac{\theta_{\mathrm{m}}}{\theta} [C_{\mathrm{m}}(t) - \overline{C}]^2 + \frac{\theta_{\mathrm{im}}}{\theta} [C_{\mathrm{im}}(t) - \overline{C}]^2 \tag{44}$$

where $\overline{C}$ is the total concentration when $t \to +\infty$. The decrease of solute concentration in the mobile phase, $C_m(t)$, as well as the concomitant increase in the immobile phase, $C_{im}(t)$, are obtained as a function of α^* by solving Eqs. (40) and (41) with the initial conditions $C_m = C_o$ and $C_{im} = 0$. Comparing by fitting the theoretical sampling variance, $\sigma^2_{C^*}(t)$ (Eq. (44)), with the measured sampling variance, Clothier et al. (1995) gave an estimation of α^*. They found that α^* was time-dependent during the duration of the experiment.

Another method to estimate θ_m and α^* was given by Jaynes et al. (1995). Rather than using a single tracer, they used a sequence of conservative anionic tracers, each being infiltrated through separate tension infiltrometers set at a given pressure head h_o, but for varying periods of time. Assuming that the initial tracer concentration in the soil is 0, and that at the sampling time, dispersion is negligible, the integration of Eq. (41) with $C_m = C_o$ and α^* considered as a constant coupled with Eq. (42) yields

$$\ln\left(1 - \frac{C^*}{C_o}\right) = -\frac{\alpha^*}{\theta_{im}} t + \ln\left(\frac{\theta_{im}}{\theta}\right) \tag{45}$$

Plotting $\ln(1 - C^*/C_o)$ vs. application time t for all of the tracers should result in a straight line with the intercept ($t = 0$) giving θ_{im} and the slope, $-\alpha^*/\theta_{im}$, providing a constant transfer rate coefficient, α^*. Jaynes and Shao (1999) modified the method without assuming $C_m = C_o$. This led to an improvement in parameter estimates, but still they were not as close as the direct application of a numerical inversion of the transport equation. They also tested the assumption of neglecting D_m through synthetic generated data.

Quadri et al. (1994) reported experiments conducted in a sand-filled box ($200 \times 200 \times 300$ mm^3) with a $\frac{1}{4}$-disc infiltrometer ($r_d = 60$ mm) placed on the soil surface at one corner of the box. They also numerically solved Eq. (1) together with the axially symmetric classical convection–dispersion equation:

$$\frac{\partial \theta C}{\partial t} = \frac{1}{r}\frac{\partial}{\partial r}\left(D\theta r \frac{\partial C}{\partial r}\right) - \frac{1}{r}\frac{\partial}{\partial r}(r q_r C) + \frac{\partial}{\partial z}\left(D\theta \frac{\partial C}{\partial z}\right) - \frac{\partial}{\partial z}(q_z C) \tag{46}$$

where q_r and q_z are the radial and vertical components of the soil water flux. Model results and observations of cumulative infiltration, soil water content and solute (bromide) profiles from removal of the disc and its replacement were found in very good agreement. They also showed that little disturbance results after refilling with a tracer solution. This has confirmed the feasibility of the method to estimate chemical transport properties of soil.

Only few attempts have been made to develop a methodology for parameter identification of reactive solute transport (Angulo-Jaramillo et al., 1995; Clothier et al., 1996). The method described by Angulo-Jaramillo et al. (1995) has demonstrated that the tension disc infiltrometer filled both with a tracer (Cl^-) and an adsorbing ion (K^+) is a suitable one for estimating the water and solute transport properties of aggregated soils. By comparing the concentration profiles of a reactive and a conservative solute, Clothier et al. (1996) were able to measure the retardation factor of the reactive solute, and then to infer its adsorption isotherm. Although very promising the method relies on severe assumptions not fully evaluated, and has to be yet tested in field conditions.

7. Some case studies results

It is beyond the scope of this paper to present an exhaustive compilation of the results obtained with the basic experimental devices described above. An emphasis is put here on some studies performed in different soil and environmental conditions. Table 1 summarizes the most relevant issues dealing with the use of tension disc and pressure ring infiltrometers as well as the corresponding references. It clearly shows that both devices, and specially the former one, have been extensively used all around the world for different purposes. Table 1 shows also a great diversity in methods of data analysis depending on the objectives of the studies and on the users as well. In the following, some results are discussed in more detail to exemplify the main methods that have been previously exposed.

7.1. Crusted soil: transient flow and inverse analysis

In the case of heterogeneous soil profiles presenting a fine layering organization, the steady-state water flow analysis based on Eq. (5), which assumes homogeneity and isotropy is generally found to be inade-

Table 1
Summary of some relevant results obtained by tension disc and pressure ring infiltrometer

Site, soil, surface cover	Aims of the study	Solute	Nb disc and size	Method of analysis	Reference
Disc infiltrometer					
Montpellier — France, loam, fallow land	Comparison of hydrodynamic properties of two contrasting soils	No	Two discs (r_d=40, 97.5 mm)	Steady flow equation (7)	Thony et al. (1991)
Las Marismas — Spain, heavy cracked clay			Two discs (r_d=40, 97.5 mm)	Steady flow equations (5), (9) and (19) and initial infiltration analysis $I(\sqrt{t})$	
Ivory coast, sandy clay with gravers	Comparison of the effect of three agricultural practices on soil surface hydraulic properties	No	Two discs S1 and S2	Steady flow and two disc analysis (Eq. (7))	Vauclin and Chopart (1992)
Maize and cotton plots with two treatments: direct sowing vs. ploughing before sowing			Ponded rings (r_d=50, 118 mm)		
Fallow ploughed 2 weeks before experiments					
Australia, red earth, wheat and lupin	Comparison of different agricultural practices	No	One disc (r_d=100 mm)	Steady flow analysis and initial infiltration analysis $I(\sqrt{t})$ (Eqs. (5), (9) and (19))	Chan and Heenan (1993)
Direct drilled vs. conventional tillage	Studying the effect of water repellency on hydraulic properties				
Stubble retained vs. stubble burnt					
NSW — Australia, sandy loam, loam, silty clay loam, wheat	Hydraulic characterization through the growing season, comparison between two tillage treatments	No	One disc (r_d=100 mm)	Steady flow and initial infiltration analysis $I(\sqrt{t})$ (Eqs. (5), (9) and (19))	Murphy et al. (1993)
New Zealand, Nicollet clay loam	Comparison between three calculation techniques and a regression method on the steady flux	No	One disc (r_d=38 mm)	Steady flow and one disc, multiple head and non-linear regression (Eq. (13))	Logsdon and Jaynes (1993)
New Zealand, Waukegan silt loam			One disc (r_d=115 mm)	Steady flow and initial infiltration analysis $I(\sqrt{t})$ (Eqs. (5), (9) and (19))	
New Zealand, Kokotan loam			Two discs (r_d=38, 115 mm)	Steady flow analysis (Eq. (7))	

Waingawa — New Zealand, Kokatan silty loam, plowed	Comparison between three calculation techniques	No	One disc (r_d=102 mm)	Steady flow and one disc multiple head (Eq. (10))	Cook and Broeren (1994)
			One disc (r_d=102 mm)	Steady flow and initial infiltration analysis $I(\sqrt{t})$ (Eqs. (5), (9) and (19))	
			Two discs (r_d=50, 102 mm)	Steady flow and two disc analysis (Eq. (7))	
New Zealand, Manawatu fine sandy loam	Evaluation of a water and solute transport model	KBr	$\frac{1}{4}$-disc (r_d=60 mm)	One disc and numerical model inversion of Eqs. (1) and (46)	Quadri et al. (1994)
TX — USA, clay of highly structured soil	Contribution of the macropore flow to infiltration of water and dye transport	No	One disc (r_d=125 mm)	Steady flow and multiple head analysis (Eq. (10))	Lin and McInnes (1995)
New Zealand, Manawatu fine sandy loam	Variation of hydraulic properties and mobile water content with the hydraulic regime, influence of the solute invasion mode	KBr	One disc (r_d=97.5 mm)	Steady flow and multiple head (Eq. (10)) with Weir approach for small radii and single tracer method (Eq. (43))	Clothier et al. (1995)
Ringelbah — France, loam with high organic matter content	Preferential flow and solute transfer on mid-mountain catchments	^{18}O	One disc S1	Transient flow (Eq. (17)) and single tracer method (Eq. (43))	Gaudet et al. (1995)
La Côte Saint André — France, Gravely sandy loam bare soil recently plowed	Variation of mobile water fraction near saturation in a structured soil	KCl	One disc S1	Transient flow equation (17) and single tracer method (Eq. (43))	Angulo-Jaramillo et al. (1996)
IA — USA, fine loamy, montmorillonite and fine silt	Spatial variability of unsaturated hydraulic parameters within a tilled field at different times	No	One disc (r_d=38 mm) at ponded and tension heads	Steady flow and one disc, multiple head and non-linear regression (Eq. (13))	Logsdon and Jaynes (1996)
HAPEX-Sahel — Niger, sand, Fallow grassland	Validation of the transient flow analysis compared to the steady flow methods	No	Two discs S1 and S2	Steady flow and two discs (Eq. (7))	Vandervaere et al. (1997)
HAPEX-Sahel — Niger, sand, Millet crops	Estimate of hydraulic properties of crusted soils		Two discs S1 and S2	Steady flow and two discs analysis (Eq. (7)) and multiple head analysis (Eq. (10))	
HAPEX-Sahel — Niger, sandy-clay loam, sedimentary and structural crusts			One side S1 and minitensiometer	Transient flow analysis (Eq. (17))	
Coria del Rio — Spain, sandy loam, maize at emergence and harvest	Temporal variation of hydraulic properties of two cultivated soils	KCl	Two discs S1 and S2	Steady state flow and two discs analysis (Eq. (7)) and single tracer method (Eq. (43))	Angulo-Jaramillo et al. (1997)
La Côte Saint André — France, Gravely sandy loam, maize at emergence and harvest					

Table 1 (*Continued*)

Site, soil, surface cover	Aims of the study	Solute	Nb disc and size	Method of analysis	Reference
USA, loam	Spatial variability of the mobile water content and the solute exchange coefficient of a field soil	Cl^-	One disc (r_d=38 mm)	NA	Casey et al. (1997)
	Evaluation of correlation between field properties	Organic tracers			
USA, Arlington fine sandy loam	Influence of disc radii upon the estimate of hydraulic conductivity	No	Four radii (r_d=27.5, 50, 75, 100 mm)	Steady flow and multiple head analysis (Eq. (10)) with Weir approach for small radii	Wang et al. (1988)
USA, Sparta sand			Three radii (r_d=32, 43.5, 172.5 mm)		
IA — USA, silty loam and fine loam, maize under no-tillage management	Scaling unsaturated hydraulic conductivity and spatial variability of different soil types and field positions	No	One disc (r_d=38 mm) at ponded and tension heads	Steady flow and multiple head analysis (Eq. (10))	Shouse and Mohanty (1998)
Ring infiltrometer					
Montpellier — France, loam, bare soil	Spatial variability of soil surface hydraulic properties	No	Ring r_d=50 mm (constant head)	Steady state flow (Eq. (28)) and transient flow (Eq. (31)) analysis	Vauclin et al. (1994)
France, liner materials, compacted silt, sand–bentonite mixture	Hydraulic characterization of slowly permeable and swelling porous materials	No	Ring r_d=50 mm (constant head and falling head)	Constant/falling head analysis of transient flow, swelling is taken into account	Gérard-Marchant et al. (1997)

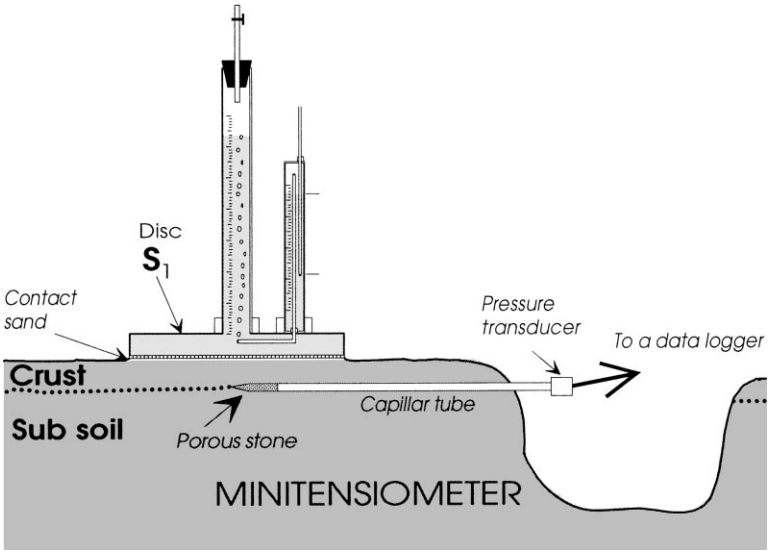

Fig. 4. Schematic representation of the experimental set-up used for measuring hydraulic properties of crusted soils (from Vandervaere et al., 1997).

quate. As shown by several authors (Hussen and Warrick, 1993; Logsdon and Jaynes, 1993), it may lead to unrealistic results including negative values of hydraulic conductivity. To overcome these difficulties a new field method has been recently proposed (Vandervaere, 1995). It is based on the simultaneous use of a disc infiltrometer and minitensiometer (Fig. 4), the transient water flow being analyzed by the three-dimensional infiltration approach (Eq. (17)) developed by Haverkamp et al. (1994) and Smettem et al. (1995). Vandervaere et al. (1997) presented comparative results obtained on different soil units of the East Central super site of the HAPEX-Sahel experiment (Goutorbe et al., 1994; Cuenca et al., 1997). In particular, the sandy-loamy-clayed soil of the lateritic plateau is characterized by the existence of large crust-covered areas of low hydraulic conductivity. The emphasis was put on two types of crust: structural (ST) and sedimentation (SED) crusts. The former are found downstream the vegetation stripes. They are formed by the sieving effect of raindrop impacts which concentrate fine particles at the bottom of the structure, while sand lies up above. SED crusts, abundant in zones of accumulation of water, are encountered upstream the vegetation stripes. They are formed by sedimentation of particles in small pools following the rain events (Casenave and Valentin, 1989; Valentin and Bresson, 1992). Infiltration tests (using discs S1 and S2, see Fig. 1) were carried out on ST and SED crust-types as well as on underlying soil (SUB) in order to estimate the contrast of conductivity between crust and subsoil. A minitensiometer (20 mm length, 2.2 mm in diameter) connected to a pressure transducer through a capillary tube (1.45 mm inner diameter) was inserted horizontally under the disc at a depth ranging from 1 cm for crusted soil to 5 cm for soils without crust (see Fig. 4). To ensure a good hydraulic contact between the disc and the soil, a sand layer was placed on the soil surface. Cumulative infiltration and the tensiometer response were monitored until the tensiometer showed an approximately constant water pressure. Before and at the end of each infiltration test, disturbed soil cores were taken for determination of initial and final gravimetric water contents, which were converted into volumetric ones through dry bulk density measured on undisturbed samples. Influence of the contact-sand layer is taken into account through the transient flow analysis (Eqs. (14) and (22)).

As an example, Fig. 5 shows the results of a typical infiltration test carried out on a ST crust with the disc S1, set at a pressure head $h_o = -10$ mm of water. Measured cumulative infiltration (Fig. 5a) and the corresponding derivative with square root of time (Fig. 5b) are used to calculate sorptivity values using

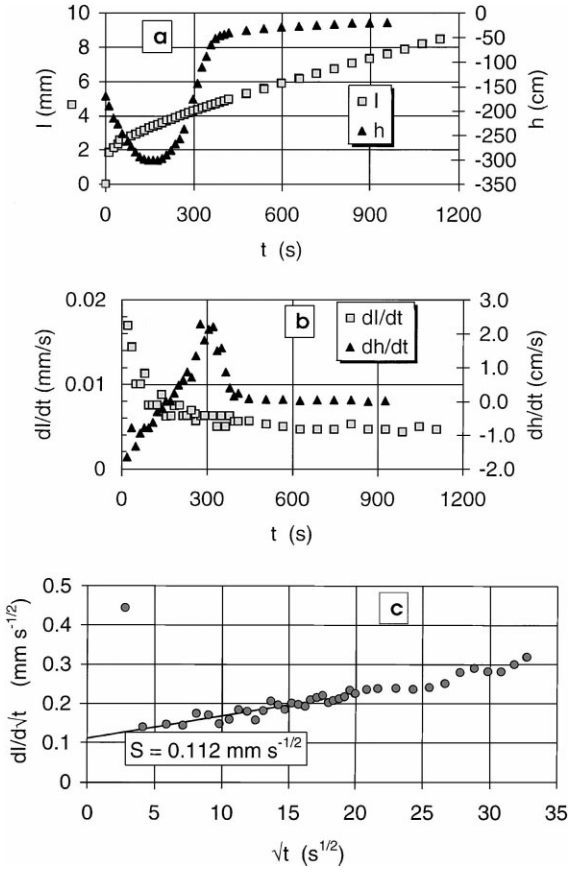

Fig. 5. Application of a tension disc infiltrometer and minitensiometer to crusted soils (tiger bush in Sahelian region, Niger) at $h_o=-10$ mm of water pressure head: (a) measured cumulative infiltration depth, I, and pressure head, h; (b) infiltration flux and rate of pressure change; (c) sorptivity estimate by Eq. (21) (from Vandervaere et al., 1997).

Eq. (22). The time of the wetting front arrival at 1 cm depth, corresponding to the maximum of dh/dt, can be identified at $t_1=300$ s. The subsequent readings being not considered in the regression analysis for Eq. (22). Fig. 6 presents the relationship between hydraulic conductivity and the soil water pressure head for the two crust-types, i.e. ST and DEC, and the subsoil (SUB) as well. As it can be seen, saturated hydraulic conductivity decreases in the crust from a factor of 3–6 as compared with the subsoils.

Another set of cumulative infiltration data were also used to test the numerical inversion of Simunek and van Genuchten (1997) (Eq. (25)) and to obtain soil hydraulic properties of a two-layered system involving a surface crust and the subsoil. First, infiltration on subsoil was analyzed to obtain the soil hydraulic characteristics (Simunek et al., 1998). This information was subsequently used to estimate the hydraulic properties of the surface crust by analyzing infiltration into the two-layered system — crust and subsoil — with the assumption that the hydraulic characteristics of the subsoil are known from the previous analysis, thus leading to estimates of the hydraulic parameters of the surface crust. The results indicate that hydraulic parameters of the subsoil are in good agreement with those obtained by parameter estimation and Wooding's (1968) analytical method (Simunek et al., 1998). In that case, saturated hydraulic conductivity of the surface crust was found to be two orders of magnitude lower than for the subsoil. Parameter estimation techniques provide an attractive alternative to the more traditional time consuming infiltration experiments which often are also limited to a relative narrow range in water content.

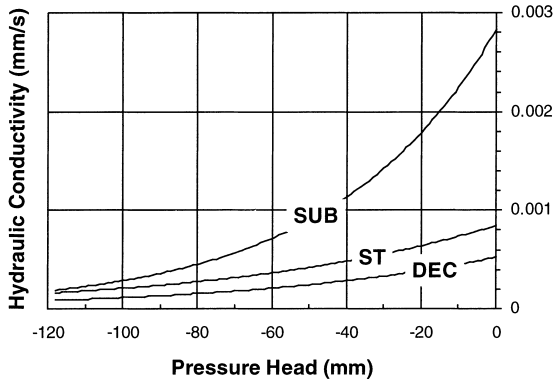

Fig. 6. Hydraulic conductivity measured by disc infiltrometer for different surface crust-types (ST=structural, DEC=sedimentary) and for the subsoil (SUB) (from Vandervaere, 1995).

7.2. *Structured soils and preferential flow: use of chemical tracers*

For structured soils, the capillary macropores play an important role in water transmission near saturation. Although they represent a small part of the porosity, they induce preferential flow paths, allowing fast transfer of an important fraction of the flow (Bouma and Wosten, 1979; Luxmoore, 1981; Beven and Germann, 1982). As pointed out by Chen and Wagenet (1992), identification of the representative

elementary volume for macroporous or structured soils is important because field observations of soil properties should be based on this volume. Few methods are available for direct determination of both unsaturated hydraulic characteristics and solute transport properties of aggregated soils with fragile structure. For field studies, the tension disc infiltrometer associated with conservative tracers has been recognized as a useful tool to the determination of both hydraulic and solute transport properties (Clothier et al., 1992, 1995, 1996; Gaudet et al., 1995; Jaynes et al., 1995; Angulo-Jaramillo et al., 1996, 1997; Casey et al., 1997, 1998; Jaynes and Shao, 1999). We report here as an example, the results dealing with infiltration tests performed with solutions of ^{18}O and Cl^- as tracers.

7.2.1. *^{18}O tracer experiment*

Infiltration test was conducted on a loamy soil with high content of organic matter. The disc S1 (Fig. 1) was chosen to characterize in the same volume the soil hydrodynamic properties and mobile water content near saturation. The mobile water content was obtained following the procedure described by Clothier et al. (1992) by using an ^{18}O ($\delta^{18}O$=53.04‰) enriched water solution as a tracer. Experiment was performed right upon the undisturbed soil surface at the imposed pressure head h_o=−30 mm of water (Fig. 7a). After penetration of the ^{18}O enriched solution to a specified depth, the disc was removed and the contact sand was rapidly scraped from underneath the disc; 75 soil samples of 30×30 mm^2 of area by 5 mm in depth were rapidly collected in an uniformly distributed pattern beneath the disc (Gaudet et al., 1995). Samples allowed determination of both total gravimetric water content (w) and ^{18}O concentration (Fig. 7b), from which mobile water content can be straightforwardly estimated through Eq. (43), where $C^*=\delta^{18}O-\delta^{18}O_n$. The initial concentration of the soil solution was $\delta^{18}O_n$=−9.11‰. Transient three-dimensional analysis of cumulative infiltration (Eq. (14)) was used to estimate both hydraulic conductivity and sorptivity, from which λ_m=519 μm was calculated by Eq. (37).

Spatial distribution of the mobile water content and the relative concentration C^*/C_o (Fig. 7b) was studied through geostatistical analysis. Experimental normalized semi-variogram of total and mobile water content

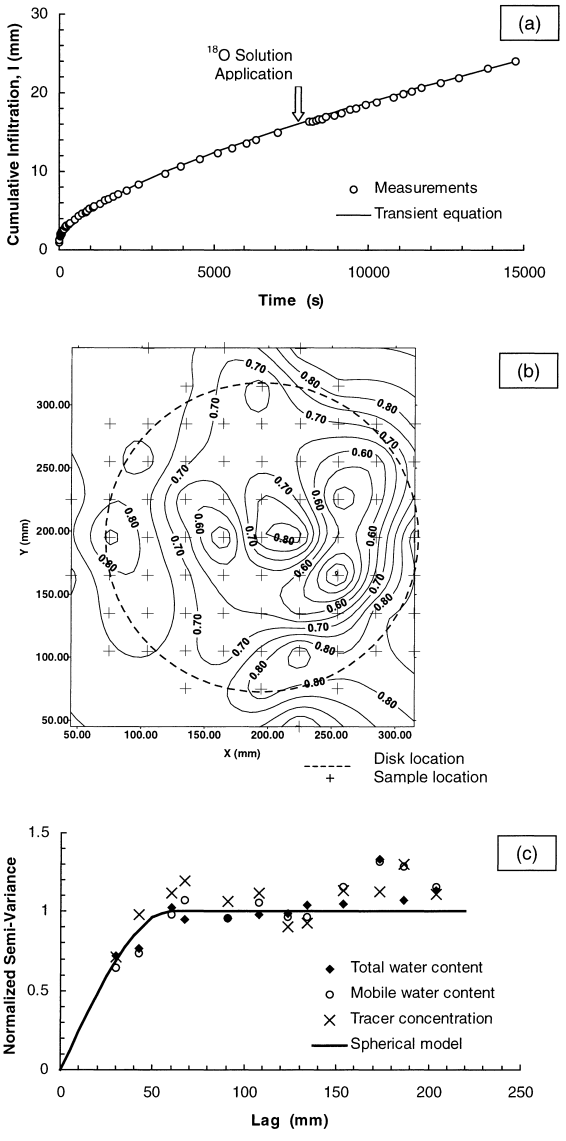

Fig. 7. Preferential flow pattern as shown by a ^{18}O tracer experiment: (a) measured infiltration data (circles) and fitted Eqs. (14)–(16); (b) kriged relative concentration of ^{18}O measured underneath the disc (r_d=125 mm); (c) normalized semi-variogram of total water content, mobile water content, and ^{18}O concentration in the soil solution (from Gaudet et al., 1995).

as well as of relative ^{18}O concentration (Fig. 7c) have been calculated as (Muñoz-Pardo et al., 1990):

$$\gamma(l) = \frac{1}{2\sigma_z^2 N(l)} \sum_{i=1}^{N(l)} [z(x_i) - z(x_i + l)]^2 \quad (47)$$

Table 2
Statistics of the soil water content and ^{18}O concentration measured beneath a tension disc infiltrometer (r_d=125 mm) after 250 min of infiltration[a]

	Number of observations	Mean	S.D.	Coefficient of variation (%)
Total soil water content by mass, w (g/g)	75	0.266	0.040	14.9
Mobile water content by mass, w_m	75	0.188	0.042	22.2
Mobile water fraction, $f=w_m/w$	75	0.707	0.144	16.1
Soil solute concentration, $C^*=\delta^{18}O$ (‰)	75	34.84	7.06	20.3

[a] From Gaudet et al. (1995).

where $N(l)$ is the number of pairs of values ($z(x_i)$, $z(x_i+l)$) obtained at location x_i and separated by a vector l, and σ_z^2 are the experimental variances of the variables of interest. Results presented in Fig. 7c show that both water content and ^{18}O concentration have the same spatial structure characterized by a range of 60 mm smaller than the radius of the disc (r_d=125 mm). This means that the whole variability at short distance is completely held within the disc size. At this scale, the large dispersion of soil water content, w, observed in Table 2 (with CV ranging from 15 to 22%) is an indicator of the existence of preferential flow pathways. This is also confirmed by the map of kriged values of the relative concentration of ^{18}O in the soil solution (Fig. 7b).

These results have been found to be in close agreement with those obtained by Lin and McInnes (1995) who used dye solution flowing from a tension disc infiltrometer. Additionally, it is worthwhile to note (Table 2) that only 70% of the total water content is mobile at the imposed water pressure head h_o=−30 mm.

7.2.2. Cl^- tracer experiment

Infiltration tests were conducted with the tension disc infiltrometer S1 filled with KCl solution in order to determine the fraction of mobile water of a recently plowed structured sandy-loam soil with a stone content of 40% (Angulo-Jaramillo et al., 1996). The applied water pressure heads h_o were chosen at −100, −60, −30 and 0 mm, and measurements were duplicated for each value of h_o. The cumulative water infiltration was recorded until apparent steady-state flow was reached. After that, water was quickly replaced by a solution of KCl, 0.1 M. After penetration of a certain depth of the solution, the disc was removed and soil samples of about 30 g of dry soil were rapidly scrapped right underneath the disc (see Fig. 3) in order to determine both the total water content (θ_o) and the chloride concentration (C^*). Fig. 8 depicts the measured distribution of both volumetric water content and relative concentration (C^*/C_m) underneath the disc at different supply water pressure heads. While the small values of the coefficient of variation of θ_o (ranging from 4 to 8%) reflect the good uniformity of wetting by the disc, measurements of C^*/C_m show a large heterogeneity in the solute entry into the soil with CVs values ranging from 41 to 84%. This indicates the existence of preferential pathways of applied solute when the hydraulic regime is established. Summary of hydrodynamic characteristics of the soil as a function of h_o are shown in Fig. 9. The strong non-linearity of both K_o (Fig. 9a) and S_o (Fig. 9b) with water pressure head shows a switch around h_o=−30 mm between a capillary dominated to a gravity dominated flow. At least a bimodal behavior of the soil may be expected. At water pressure close to zero the flow is controlled by the macroporosity. The soil has high values of hydraulic conductivity, sorptivity and mean functional pore size λ_m=970 μm (Eq. (37)). When water pressure decreases, the water flow becomes controlled by the mesoporosity and all the variables decrease gradually, and some of them such as K_o drastically. It is worthwhile to point out that some other results (Sauer et al., 1990; Ankeny et al., 1991; Clothier et al., 1995; Jarvis and Messing, 1995) have also suggested the existence of a break-point on the $K_o(h_o)$ relationship located between −60 and −25 mm of water pressure head.

The dependence of the mobile water content fraction, $f=\theta_m/\theta_o=C^*/C_o$ calculated by Eq. (43), on λ_m is presented in Fig. 9d. Angulo-Jaramillo et al. (1996)

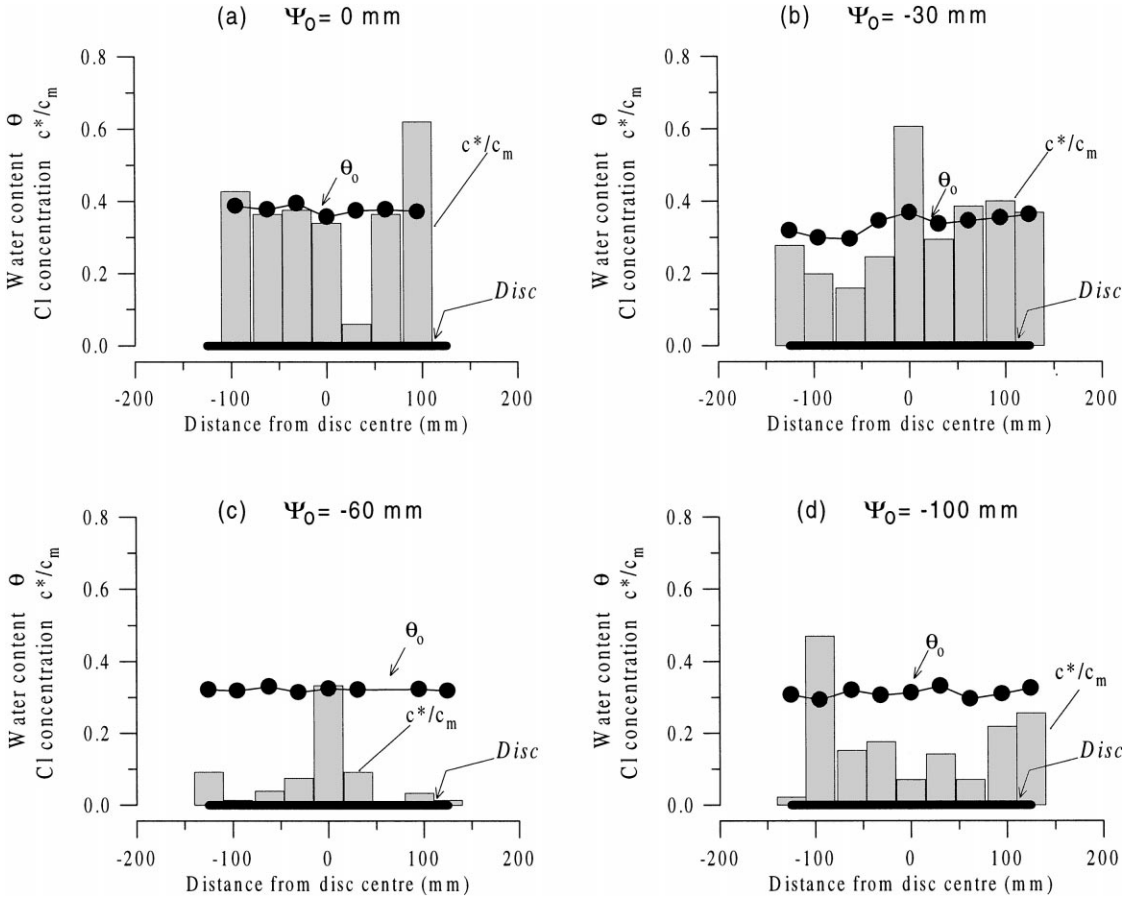

Fig. 8. Volumetric water content, θ_o, and relative concentration of Cl^- (C^*/C_m) measured underneath a disc (r_d=125 mm) at different supply water pressure heads (from Angulo-Jaramillo et al., 1996).

have suggested to approximate the data by the following hyperbolic s-shaped curve:

$$\frac{f(\lambda_m)-f_m}{f_M-f_m}=\frac{1}{[1+(\lambda_m^*/\lambda_m)^a]^c} \quad (48)$$

where f_m represents the mobile water fraction in the microporosity or in the soil matrix hydraulically active at water pressure heads smaller than -60 mm, f_M is the value of the mobile water fraction of the soil including both micro- and macroporosity for $h_o>-30$ mm, f_m, f_M, λ_m^*, a and c are fitting parameters (with $c=1-2/a$ and $0<c<1$). The parameter λ_m^* can be interpreted as a mean effective pore size that discriminates capillary-dominated to gravity-dominated flow for given initial and boundary conditions (Fig. 9d). The proposed relationship (Eq. (48)) or its equivalent $f(\Delta\theta K_o/S_o^2)$ provides a continuous dynamic change of the mobile water content ratio from the microporosity to the macroporosity.

7.3. Temporal variability of soil hydraulic properties

While it is usually considered in most of the water and solute models that soil surface characteristics are time constant, it is well known that in fact they undergo temporal changes induced for instance by irrigation and tillage practices, rain and wind weathering, biological activity which can drastically modify the soil structure (Chan and Heenan, 1993; Kutilek et al., 1993; Messing and Jarvis, 1993; Murphy et al., 1993; Somaratne and Smettem, 1993; Logsdon and Jaynes, 1996; Heddadj and Gascuel-Odoux, 1999).

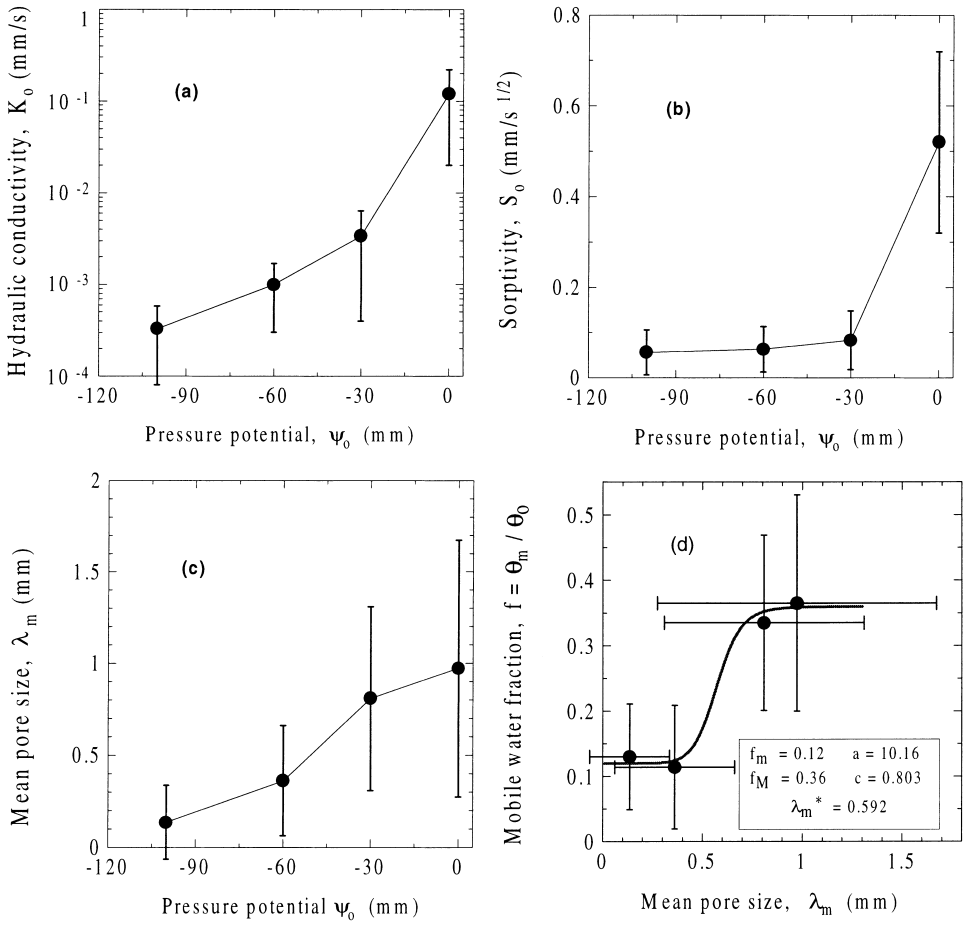

Fig. 9. Hydraulic properties of a field soil: (a) hydraulic conductivity; (b) sorptivity; (c) functional mean pore size radius as a function of the supply water pressure head; (d) variation of the mobile water fraction as a function of mean pore size and fitting curve by Eq. (48). The bars correspond to experimental standard deviation (from Angulo-Jaramillo et al., 1996).

We give here an example of application of tension disc infiltrometers to quantify temporal changes in hydrodynamic properties of two soils: a sandy soil located in Coria del Rio (Spain) and the stony sandy loam soil of La Côte Saint André (France) (Angulo-Jaramillo et al., 1997). Both soils were cropped with maize and underwent conventional tillage and different irrigation practices, namely furrow irrigation and gun irrigation, respectively. The mobile water content was also determined by the tension infiltrometer S1 (Fig. 1) filled with a chloride tracer. Measurements were made at two dates: (i) at emergence stage (period 1), before the irrigation period, and (ii) at the end of the growing season (period 2), after irrigation stopped. The corresponding results are presented in Fig. 10 for the two sites and the two periods. The sandy soil under furrow irrigation (Site A) shows drastic reduction of both K_o and S_o (Fig. 10a and b) between period 1 and 2. It may be explained by the soil compaction since the bulk density varied from 1.36 to 1.55 Mg m^{-3}. At saturation, the characteristic pore size λ_m of Site A decreases dramatically between the two periods (Fig. 10c). This might be explained by some fraction of the smaller pores becoming isolated when the seedbed settled, following the surface crust formation under furrow irrigation (Le Bissonnais et al., 1989).

A strong non-linearity in the hydraulic conductivity was found for the soil of Site B, with no significant

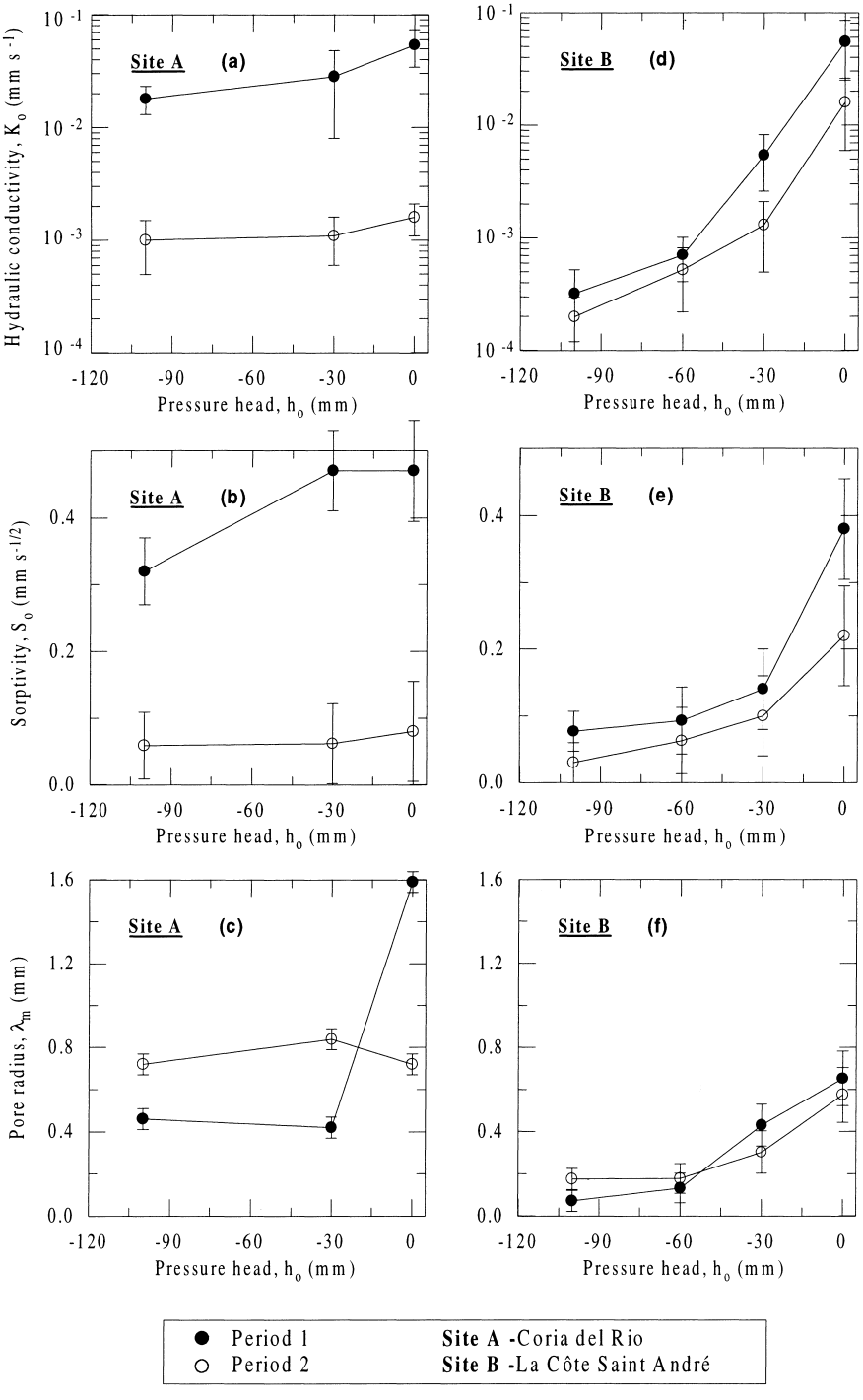

Fig. 10. Hydrodynamic characterization of two sites for period 1 (emergence of maize, before irrigation) and 2 (at harvest, after irrigation): variation with the imposed pressure head h_o of the hydraulic conductivity (a, d), sorptivity (b, e), and mean pore size (c, f) (from Angulo-Jaramillo et al., 1997).

change in this behavior during the growing season (Fig. 10d and e). The differences of K_o values between the two periods of measurements are much less important than at Site A. Nevertheless, some reduction in K_o is observed. The sorptivity values of the second period are also lower than during the first one (Fig. 10e). The decrease of both K_o and S_o are significant, and more important for $h_o > -30$ mm. There was no significant change in the bulk density, i.e. 1.22–1.20 Mg m^{-3} between the two periods, respectively. The values of the mean pore radius (λ_m) are presented in Fig. 10f. During period 1, functional pores have small radii (0.07–0.13 mm) for $h_o < -60$ mm, indicating that the flux is controlled by the aggregates of the finer fraction. For $-60 < h_o < 0$ mm, λ_m increases gradually (0.43–0.65 mm) following an increase in the conductivity and the sorptivity. The coarse material at this site appears responsible for the important network of preferential flow paths in period 1. During period 2, the variation in λ_m at site B was less significant than that at site A. Nevertheless, λ_m increases for $h_o < -60$ mm and decreases for $h_o > -30$ mm. This result probably comes from a homogenization of the functioning pores around a mean value of 0.31 mm. It appears that during period 2 there is a lack of interconnected small pores, creating both lower K_o and S_o for pressure heads $-100 < h_o < -30$ mm, and leading to higher values of λ_m in period 2. Secondly, it seems that there is either a reduction in the macroporosity at the coarse–fine interface material in agreement with the reduction of K_o, and an isolation of a fraction of the small pores in agreement with the reduction of S_o. Thus the coarse material of the soil surface at Site B appears to form a rigid skeleton, yet with a macroporosity that facilitates rapid water transmission into the soil. During this phase, the fine fraction changes its structural pattern from a well-interconnected microporous network at emergence (period 1) to a poorly interconnected one at harvest time (period 2). These changes in the porous network were also partially corroborated by the increase of the mobile water content during the growing season (Fig. 11), as discussed by Angulo-Jaramillo et al. (1997).

7.4. Spatial variability of hydraulic conductivity

Due to the inherent variability of soil hydraulic properties, a pure deterministic approach is very questionable for describing the unsaturated behavior of fields (for agricultural or engineering purposes) or watersheds (for hydrologic or environmental studies). This implies that both a statistical description of the parameters governing soil transfer characteristics, and stochastic models of unsaturated flow should be considered (Nielsen et al., 1973; Sharma et al., 1980; Yeh et al., 1985a,b,c; Mantoglou and Gelhar, 1987; White and Sully, 1992; Kutilek et al., 1993; Kutilek and Nielsen, 1994). The empirical exponential relationship $K(h)$ (Eq. (11)) has been extensively used in deterministic models. A great advantage of this representation is that only one parameter, the so-called ''alpha parameter'' is required to describe the unsaturated hydraulic behavior of the soil, while the saturated hydraulic conductivity, K_{fs}, is used as a scale factor for the near-saturated condition as shown by Shouse and Mohanty (1998). As pointed out by White et al. (1992), $\alpha = \lambda_c^{-1}$ (see Eq. (36)) is a measure of the capillary forces relative to the gravity ones, and it is related to the internal pore geometry of the soil. If many field studies have shown that K_{fs} may be considered as log-normally distributed, the statistical distribution of α is generally less known.

Due to their portability, disc and ring infiltrometers are valuable tools to investigate both K_{fs} and α statistical distributions. Analysis of positive water pressure head infiltration from ring infiltrometer, namely Guelph Pressure Infiltrometer (Reynolds and Elrick, 1990; Elrick and Reynolds, 1992a,b), gives directly estimates of K_{fs} and α. On a bare agricultural soil of the Domaine of Lavalette near Montpellier (south of France), 32 infiltration measurements were made at each node of an 4 m×8 m grid for three hydraulic heads 60, 160 and 255 mm (Vauclin et al., 1994). K_{fs} and ϕ_m values were obtained by using the two head simultaneous equation procedure (Eq. (28)) applied to the steady-state flow rates. The α values were calculated by Eq. (30). The resulting cumulative probability distributions of K_{fs} and α (Fig. 12) exhibit a systematic departure from the normal distribution, whereas departures for the log-normal are much smaller and less systematic. On the basis of Student's t-test, and on the analysis of third and four moments of the distributions (Vauclin et al., 1982; Vauclin et al., 1983), the normal distribution was rejected (at the 95% level), whereas the log-normal one appeared more acceptable for both K_{fs} and α. White and Sully (1992) presented

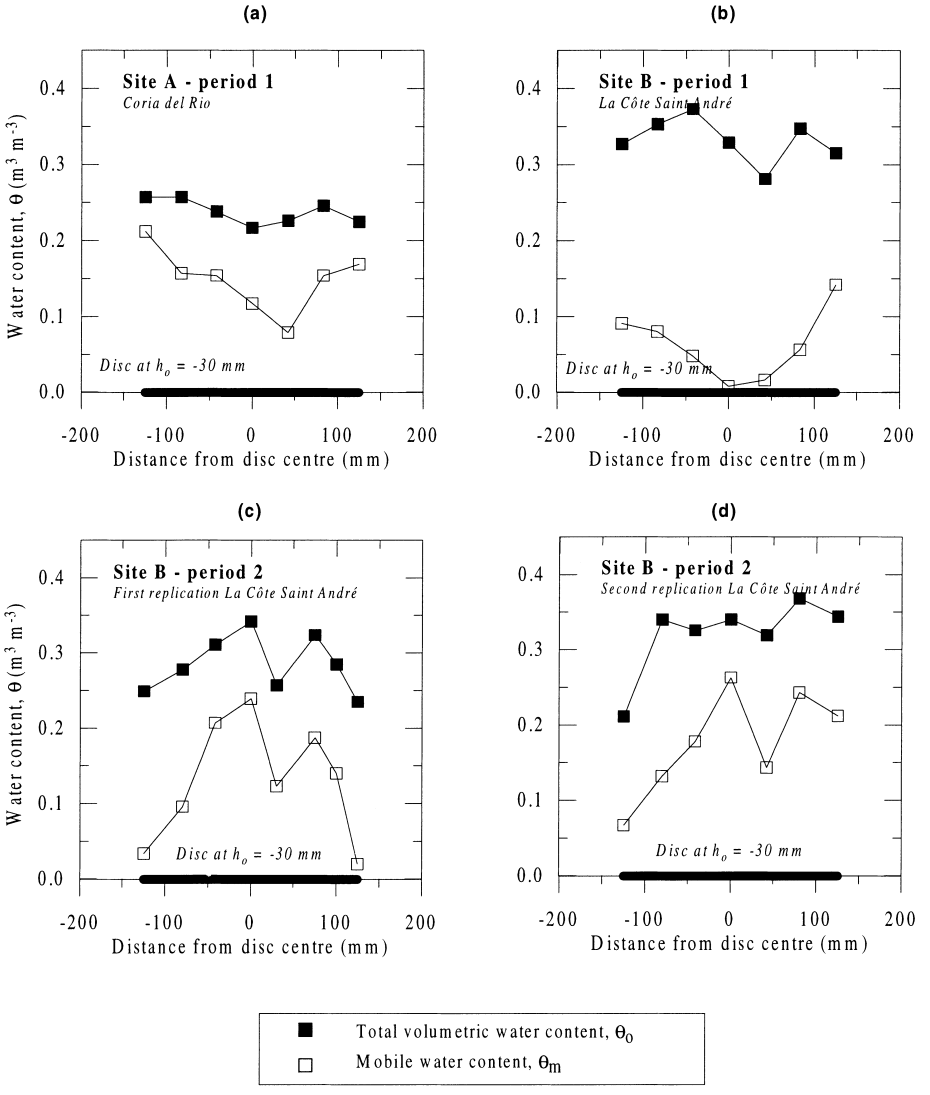

Fig. 11. Mobile and total volumetric water content sampled from the soil-surface along the disc infiltrometer (r=125 mm and h_o=−30 mm) at the end of infiltration with KCl solution. Period 1 (emergence of maize, before irrigation) in Coria del Rio, Spain (a) and La Cote Saint André, France (b); and period 2 (harvest, after irrigation), two replications (c, d) at La Côte Saint André, France (from Angulo-Jaramillo et al., 1997).

results which indicate that also K_{fs} and α are better described by a log-normal distribution.

Large nugget effect of semi-variograms (Fig. 13) corresponds to the spatial variability that occurs within distances shorter than the sampling intervals (4 m×8 m) and to experimental uncertainties. It appears that the α values fluctuate more at small distances than K_{fs}. This might be due to greater influence of capillary macropores on α as compared to K_{fs}. A sill greater than unity was observed for the normalized semi-variograms after 25 m for K_{fs} and about 20 m for α. Field results presented here do not of course guarantee that the distributions of both K_{fs} and α are log-normal. Goodness of fit tests need several hundreds of observations to really decide on the appropriate distribution function, not always easily obtainable in the field. However, the results suggest that both K_{fs} and α are better described by the log-normal distribution than a

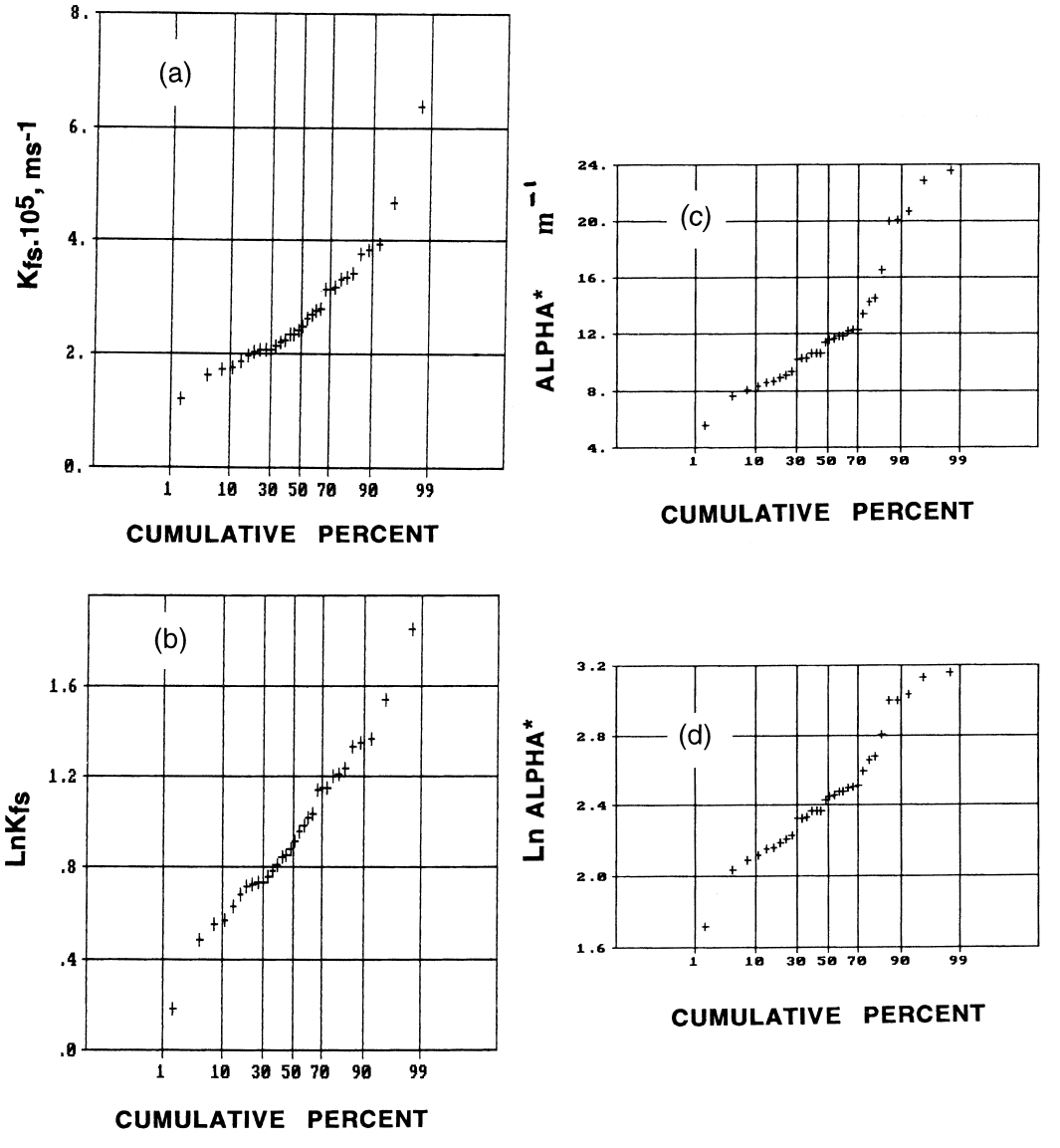

Fig. 12. Cumulative probability distribution function of 32 values of K_{fs} (a), $\ln(K_{fs})$ (b), α (c), and $\ln(\alpha)$ (d), obtained by a pressure ring infiltrometer (from Vauclin et al., 1994).

normal one. Because K_{fs} and α are related to the same pore geometry and both present a spatial structure, it is not surprising that their correlation exhibits some spatial persistence as well, as it can be seen from the cross covariances shown in Fig. 13. The results reinforce the need to consider partial correlation in field-scale hydrologic models as it has been suggested but not explored by Tiejte and Richter (1992), or more recently investigated by Shouse and Mohanty (1998). It is also noticed that the unknown field saturated hydraulic conductivity (and the unknown α) is the sum of the estimated value K_{fs} (i.e. α) and the error due to the approximate nature of the estimation. Since this error does not necessarily follow the same probability distribution function as the real value, various probability functions of K_{fs} (i.e. of α) could be obtained even for the same data set

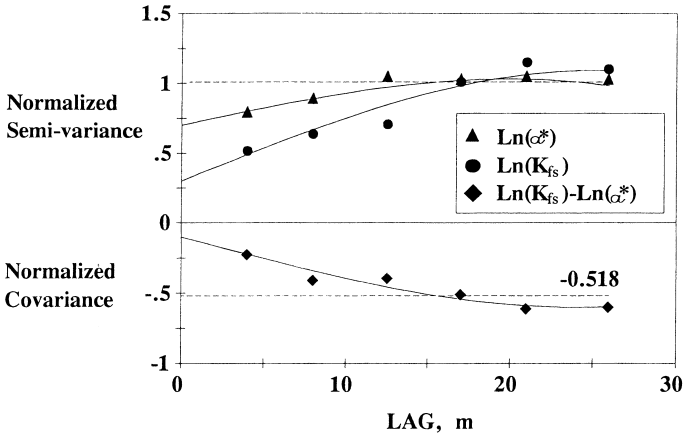

Fig. 13. Experimental semi-variograms and cross semi-variograms. Solid lines represent the theoretical spherical model fitting the experimental values given in Fig. 12 (from Vauclin et al., 1994).

when K_{fs} is evaluated by different approximations. In such case, log-normal distribution of K_{fs} or α would be just one possible deviation from the normal distribution (Nielsen et al., 1996).

8. Concluding remarks

Unsaturated hydraulic properties are key inputs in understanding and modeling the dynamic processes of water and solute movement in the vadose zone. Methods available for obtaining these parameters are often difficult to use and time consuming. This non-exhaustive review has shown that tension disc and pressure ring infiltrometers are useful instruments that offer a simple and fast means of estimating soil hydraulic properties and structural characteristics based on infiltration measurements at the soil surface when combined with appropriate theoretical principles or procedures briefly summarized in the paper. These include the measurement of both initial and final soil water content, and the infiltration rate at the early infiltration stage, the steady infiltration rates either at two or more locations, or at two or more supply water pressure heads, with an assumed $K(h)$ form with continuous or piecewise parameters. Other methods include accurate measurements of transient multidimensional infiltration rate and numerical inversion of the flow equation. It has also been shown that such techniques are suitable to estimate preferential flow parameters in the field as well as those related to solute transport.

However, there are no panaceas in soil physics, and tension disc and ring infiltrometer, as well, also have limitations; most of them being associated with the simplifying assumptions of the analysis used to infer soil hydraulic properties from water and solute flow measurements. In addition, other problems are either inherent in the measurement procedures themselves or arise from difficult soils, such as hydrophobic, swelling materials. When measurements are made at supply water pressure heads close to zero, discs must be well leveled, otherwise the pressure will vary across the supply surface. Furthermore, the weight of the infiltrometer may induce collapse of the soil leading to negative values of hydraulic conductivity. While analysis of flow requires the knowledge of the volumetric soil water content in equilibrium with the imposed water pressure head, errors can arise in sampling those values because of the small sampling depth required and the fact that the dry bulk density should be known. It may be mentioned that the use of small time domain reflectometry probes may solve this problem, as it has been recently shown by Vogeler et al. (1996) or Wang et al. (1998).

Despite these limitations, it is thought that tension disc and ring infiltrometers are very suitable techniques for determining in situ soil hydraulic properties and particularly surface soils which are very complex materials.

Acknowledgements

The authors thank Miroslav Kutilek for his helpful comments and suggestions regarding earlier version of this paper.

References

Angulo-Jaramillo, R., Gaudet, J.P., Thony, J.L., Vandervaere, J.P., Vauclin, M., Clothier, B.E., 1995. The mobile water content in an aggregated unsaturated soil. In: Alonso, E.E., Delage, P., Balkena, A.A. (Eds.), Unsaturated Soils. Proceedings of the First International Conference on Unsaturated Soils, UNSAT '95, Vol. 1. Rotterdam, Paris, September 6–8, pp. 349–354 (ISBN 90 5410 584 4).

Angulo-Jaramillo, R., Gaudet, J.P., Thony, J.L., Vauclin, M., 1996. Measurement of hydraulic properties and mobile water content of a field soil. Soil Sci. Soc. Am. J. 60, 710–715.

Angulo-Jaramillo, R., Moreno, F., Clothier, B.E., Thony, J.L., Vachaud, G., Fernandez-Boy, E., Cayuela, J.A., 1997. Seasonal variation of hydraulic properties of soils measured using a tension disc infiltrometer. Soil Sci. Soc. Am. J. 61, 27–32.

Ankeny, M.D., Kaspar, T.C., Horton, R., 1988. Design for an automated infiltrometer. Soil Sci. Soc. Am. J. 52, 893–896.

Ankeny, M.D., Ahmed, M., Kaspar, T.C., Horton, R., 1991. Simple field method determining unsaturated hydraulic conductivity. Soil Sci. Soc. Am. J. 55, 467–470.

Beven, K., Germann, P., 1982. Macropores and water flow in soils. Water Resour. Res. 18, 1311–1325.

Bonnell, M., Williams, J., 1986. The two parameters of the Philip infiltration equation: their properties and spatial and temporal heterogeneity in a red earth of tropical semi-arid Queensland. J. Hydrol. 87, 9–31.

Bouma, J., Wosten, J.H.M., 1979. Flow patterns during extended saturated flow in two undisturbed swelling clay soils with different macropores. Soil Sci. Soc. Am. J. 43, 16–22.

Brutsaert, W., 1979. Universal constants for scaling the exponential soil water diffusivity. Water Resour. Res. 15, 481–483.

Casenave, A., Valentin, C. (Eds.), 1989. Les états de surface en zone sahélienne. ORSTOM, Paris, 229 pp.

Casey, F.X.M., Logsdon, S.D., Horton, R., Jaynes, D.B., 1997. Immobile water content and mass exchange coefficient of a field soil. Soil Sci. Soc. Am. J. 61, 1030–1036.

Casey, F.X.M., Logsdon, S.D., Horton, R., Jaynes, D.B., 1998. Measurements of field soil hydraulic and solute transport parameters. Soil Sci. Soc. Am. J. 62, 1172–1178.

Chan, K.Y., Heenan, D.P., 1993. Surface hydraulic properties of a red earth under continuous cropping with different management practices. Aust. J. Soil Res. 31, 13–24.

Chen, C., Wagenet, R.J., 1992. Simulation of water and chemicals in macropore soils. Part 1. Representation of the equivalent macropore influence and its effect on soil water flow. J. Hydrol. 130, 105–126.

Clausnitzer, V., Hopmans, J.W., 1995. Non-linear parameter estimation: LM_OPT. General-purpose optimization code based on the Levenberg–Marquartd algorithm. Land, Air and Water Resources Paper No. 100032, University of California, Davis, CA.

Clausnitzer, V., Hopmans, J.W., Starr, J.L., 1998. Parameter uncertainty analysis of common infiltration models. Soil Sci. Soc. Am. J. 62, 1477–1487.

Clothier, B.E., Smettem, K.R.J., 1990. Combining laboratory and field measurements to define the hydraulic properties of soil. Soil Sci. Soc. Am. J. 54, 299–304.

Clothier, B.E., Kirkham, M.B., McLean, J.E., 1992. In situ measurement of the effective transport volume for solute moving through soil. Soil Sci. Soc. Am. J. 56, 733–736.

Clothier, B.E., Heng, L., Magesan, G.N., Vogeler, I., 1995. The measured mobile-water content of an unsaturated soil as a function of hydraulic regime. Aust. J. Soil Res. 33, 397–414.

Clothier, B.E., Magesan, G.N., Han, L., Vogeler, I., 1996. In situ measurement of the solute adsorption isotherm using a disc permeameter. Water Resour. Res. 32, 771–778.

Coats, K.H., Smith, B.D., 1964. Dead-end pore volume and dispersion in porous media. Soc. Pet. Eng. J. 4, 73–84.

Cook, F.J., Broeren, A., 1994. Six methods for determining sorptivity and hydraulic conductivity with disc permeameters. Soil Sci. 157 (1), 2–11.

Cuenca, R.H., Brouwer, J., Chanzy, A., Droogers, P., Galle, S., Gaze, S., Sicot, M., Stricker, H., Angulo-Jaramillo, R., Boyle, S.A., Bromley, J., Chebhouni, A.G., Cooper, J.D., Dixon, A.J., Fies, J.C., Gandah, M., Gaudu, J.C., Laguerre, L., Soet, M., Stewart, H.J., Vandervaere, J.P., Vauclin, M., 1997. Soil measurements during the HAPEX-Sahel intensive observation period, J. Hydrol. Spec. Issue HAPEX-Sahel (188/189), 224–266.

Elrick, D.E., Reynolds, W.D., 1992a. Infiltration from constant head well permeameters and infiltrometers. In: Topp, G.C., et al. (Eds.), Advances in Measurement of Soil Physical Properties: Bringing Theory into Practice. Soil Sci. Soc. Am. Spec. Publ. 30. SSSA, Madisson, WI, pp. 1–24.

Elrick, D.E., Reynolds, W.D., 1992b. Methods for analyzing constant head well permeameter data. Soil Sci. Soc. Am. J. 56, 320–323.

Elrick, D.E., Parkin, G.W., Reynolds, W.D., Fallow, D.J., 1995. Analysis of early-time and steady-state single-ring infiltration under falling head condition. Water Resour. Res. 31, 1883–1894.

Fallow, D.J., Elrick, D.E., Reynolds, W.D., Baumgartner, M., Parkin, W., 1994. Field measurement of hydraulic conductivity in slowly permeable materials using early-time infiltration measurements in unsaturated media. In: Daniel, D.E., Trautwein, S.J. (Eds.), Hydraulic Conductivity and Waste Contaminant Transport in Soil, ASTM STP 1142. American Society for Testing Materials, Philadelphia, PA, pp. 375–389.

Gardner, W.R., 1958. Some steady-state solutions of the unsaturated moisture flow equation with application to evaporation from a water table. Soil Sci. 85, 228–232.

Gaudet, J.P., Jégat, H., Vachaud, G., Wierenga, P.J., 1977. Solute transfer with exchange between mobile and stagnant water

through unsaturated sand. Soil Sci. Soc. Am. J. 41 (4), 665–671.

Gaudet, J.P., Angulo-Jaramillo, R., Thony, J.L., Vauclin, M., Ladouche, B., Bariac, T., Huon, S., Ambroise, B., Auzet, A.V., 1995. Mesures in situ de la fraction immobile de l'eau du sol avec de l'eau enrichie en ^{18}O dans un infiltromètre à succion contrôlée. In: Proceedings of the Conference on Isotopes on Water Resource Management, Vol. 1. AIEA-SM-336/130P, Vienna, March, 20–24, 1995, pp. 28–35

Gérard-Marchant, P., Angulo-Jaramillo, R., Haverkamp, R., Vauclin, M., Groenevelt, P., Elrick, D.E., 1997. Estimating the hydraulic conductivity of slowly permeable and swelling materials from single-ring experiments. Water Resour. Res. 33 (6), 1375–1382.

Goutorbe, J.P., Lebel, T., Tinga, A., Bessemoulin, P., Brouwer, J., Dolman, A.J., Engman, E.T., Gash, J.H.C., Hoepffner, M., Kabbat, P., Kerr, Y.H., Monteny, B., Prince, S., Said, F., Sellers, P., Wallace, J.S., 1994. HAPEX-Sahel: a large scale study of land–atmosphere interactions in the semi-arid tropics. Ann. Geophys. 12, 53–64.

Haverkamp, R., Kutilek, M., Parlange, J.Y., Rendon, L., Krejca, M., 1988. Infiltration under ponded conditions. Part 2. Infiltration equations tested for parameter time-dependence and predictive use. Soil Sci. 145 (5), 317–329.

Haverkamp, R., Ross, P.J., Smettem, K.R.J., Parlange, J.Y., 1994. Three dimensional analysis of infiltration from the disc infiltrometer. Part 2. Physically based infiltration equation. Water Resour. Res. 30, 2931–2935.

Heddadj, D., Gascuel-Odoux, C., 1999. Topographic and seasonal variations of unsaturated hydraulic conductivity as measured by tension disc infiltrometers at the field scale. Eur. J. Soil Sci. 50, 275–283.

Hussen, A.A., Warrick, A.W., 1993. Alternative analysis of hydraulic data from the disc tension infiltrometers. Water Resour. Res. 29, 4103–4108.

Jarvis, N.J., Messing, I., 1995. Near-saturated hydraulic conductivity in soils of contrasting texture measured by tension infiltrometers. Soil Sci. Soc. Am. J. 59, 27–34.

Jaynes, D.B., Shao, M., 1999. Evaluation of a simple technique for estimating two-domain transport parameters. Soil Sci. 164 (2), 82–91.

Jaynes, D.B., Logsdon, S.D., Horton, R., 1995. Field method for measuring mobile/immobile water content and solute transfer rate coefficient. Soil Sci. Soc. Am. J. 59, 352–356.

Kutilek, M., Nielsen, D.R., 1994. Soil Hydroloey. Catena Verlag, Cremlingen, 370 pp. (ISBN 3-923381-26-3).

Kutilek, M., Kuraz, V., Krejca, M., 1993. Measurement time and spatial variability of field infiltration. Int. Agrophys. 7, 133–140.

Le Bissonnais, Y., Bruand, A., Jamagne, M., 1989. Laboratory experimental study of soil crusting: relation between aggregate breakdown mechanisms and crust structure. Catena 16, 377–392.

Lin, H.S., McInnes, K.J., 1995. Water flow in clay soil beneath a tension infiltrometer. Soil Sci. 159 (6), 375–382.

Logsdon, S.D., 1997. Transient variation in the infiltration rate during measurement with tension infiltrometers. Soil Sci. 162 (4), 233–241.

Logsdon, S.D., Jaynes, D.B., 1993. Methodology for determining hydraulic conductivity with tension infiltrometers. Soil Sci. Soc. Am. J. 57, 1426–1431.

Logsdon, S.D., Jaynes, D.B., 1996. Spatial variability of hydraulic conductivity in a cultivated field at different times. Soil Sci. Soc. Am. J. 60, 703–709.

Luxmoore, R.J., 1981. Micro-, meso-, and macroporosity of soil. Soil Sci. Soc. Am. J. 45, 671–672.

Mantoglou, A., Gelhar, L.W., 1987. Stochastic modeling of large-scale transient unsaturated flow systems. Water Resour. Res. 23, 37–46.

Marquardt, D.W., 1963. An algorithm for least square estimation of non linear parameters. SIAM J. Appl. Math. 11, 431–441.

Messing, I., Jarvis, N., 1993. Temporal variation in the hydraulic conductivity of a tilled clay soil as measured by tension infiltrometers. J. Soil Sci. 44, 11–24.

Muñoz-Pardo, J., Ruelle, P., Vauclin, M., 1990. Spatial variability of an agricultural field: geostatistical analysys of soil texture, soil moisture and yield components of two rainfed crops. Catena 17, 369–381.

Murphy, B.W., Koen, T.B., Jones, B.A., Huxedurp, L.M., 1993. Temporal variation of hydraulic properties of some soils with fragile structure. Aust. J. Soil Res. 31, 179–197.

Nielsen, D.R., Biggar, J.W., Erh, K.T., 1973. Spatial variability of field measured soil properties. Hilgardia 42, 215–259.

Nielsen, D.R., Kutilek, M., Parlange, M.B., 1996. Surface soil water content regimes: opportunities in soil science. J. Hydrol. 184, 35–55.

Perroux, K.M., White, I., 1988. Designs for disc permeameters. Soil Sci. Soc. Am. J. 52, 1205–1215.

Philip, J.R., 1957a. Numerical solution of equations of the diffusion type with diffusivity concentration-dependent. Aust. J. Phys. 10, 29–42.

Philip, J.R., 1957b. The theory of infiltration. Part 4. Sorptivity and algebraic infiltration equations. Soil Sci. 84, 257–264.

Philip, J.R., 1969. Theory of infiltration. Adv. Hydrosci. 5, 215–296.

Philip, J.R., 1985. Reply to ''Comments on steady infiltration from spherical cavities''. Soil Sci. Soc. Am. J. 19, 788–789.

Philip, J.R., 1986. Linearized unsteady multidimensional infiltration. Water Resour. Res. 22, 1717–1727.

Quadri, B.M., Clothier, B.E., Angulo-Jaramillo, R., Vauclin, M., Green, S.R., 1994. Axisymmetric transport of water and solute underneath a disc permeameter. Experiments and a numerical model. Soil Sci. Soc. Am. J. 58 (3), 696–703.

Reichardt, K.D., Nielsen, D.R., Biggar, J.W., 1972. Scaling of horizontal infiltration into homogeneous soils. Soil Sci. Soc. Am. Proc. 36, 240–245.

Reynolds, W.D., Elrick, D.E., 1990. Ponded infiltration from a single ring. Part 1. Analysis of steady flow. Soil Sci. Soc. Am. J. 54, 1233–1241.

Reynolds, W.D., Elrick, D.E., Clothier, B.E., 1985. The constant head well permeameter: effect of unsaturated flow. Soil Sci. 139, 172–180.

Sauer, T.J., Clothier, B.E., Daniel, T.C., 1990. Surface measurements of the hydraulic properties of a tilled and untilled soil. Soil Till. Res. 15, 359–369.

Scotter, D.R., Clothier, B.E., Harper, E.R., 1982. Measuring saturated hydraulic conductivity and sorptivity using twin rings. Aust. J. Soil Res. 20, 295–304.

Sharma, M.L., Gander, G.A., Hunt, C.G., 1980. Spatial variability of infiltration in a watershed. J. Hydrol. 45, 101–122.

Shouse, P.J., Mohanty, B.P., 1998. Scaling of near-saturated hydraulic conductivity measured using disc infiltrometers. Water Resour. Res. 34 (5), 1195–1205.

Simunek, J., van Genuchten, M.Th., 1996. Estimating unsaturated soil hydraulic properties from tension disc infiltrometer data by numerical inversion. Water Resour. Res. 32, 2683–2696.

Simunek, J., van Genuchten, M.Th., 1997. Parameter estimation of soil hydraulic properties from multiple tension disc infiltrometer data. Soil Sci. 162, 383–398.

Simunek, J., Angulo-Jaramillo, Rh., Schaap, M.G., Vandervaere, J.P., van Genuchten, M.T., 1998. Using an inverse method to estimate hydraulic properties of crusted soils from tension-disc infiltrometer data. Geoderma 86, 61–81.

Smettem, K.R.J., Clothier, B.E., 1989. Measuring unsaturated sorptivity and hydraulic conductivity using multi-disc permeameters. J. Soil Sci. 40, 563–568.

Smettem, K.R.J., Parlange, J.Y., Ross, P.J., Haverkamp, R., 1994. Three-dimensional analysis of infiltration from the disc infiltrometer. Part 1. A capillary-based theory. Water Resour. Res. 30, 2925–2929.

Smettem, K.R.J., Ross, P.J., Haverkamp, R., Parlange, J.Y., 1995. Three-dimensional analysis of infiltration from the disc infiltrometer. Part 3. Parameter estimation using a double-disc tension infiltrometer. Water Resour. Res. 31, 2491–2495.

Somaratne, N.M., Smettem, K.R.J., 1993. Effect of cultivation and raindrop impact on the surface hydraulic properties of an alfisol under wheat. Soil Till. Res. 26, 115–125.

Thony, J.L., Vachaud, G., Clothier, B.E., Angulo-Jaramillo, R., 1991. Field measurements of the hydraulic properties of soil. Soil Technol. 4, 111–123.

Tiejte, O., Richter, O., 1992. Stochastic modeling of the unsaturated water flow using autocorrelated spatially variable hydraulic parameters. Modeling Geo-biosphere 1, 163–183.

Turner, N.C., Parlange, J.Y., 1974. Lateral movement at the periphery of a one-dimensional flow of water. Soil Sci. 118, 70–77.

Valentin, C., Bresson, L.M., 1992. Morphology, genesis and classification of surface crusts in loamy and sandy soils. Geoderma 55, 225–245.

Vandervaere, J.P., 1995. Caractérisation hydrodynamique du sol in-situ par infiltrométrie à disques. Analyse critique des régimes pseudopermanents, methodes transitoires et cas de sols encroutés. Ph.D. Thesis. Université Joseph Fourier, Grenoble 1, 326 pp.

Vandervaere, J.P., Peugeot, C., Vauclin, M., Angulo-Jaramillo, R., Lebel, T., 1997. Estimating hydraulic conductivity of crusted soils using disc infiltrometers and minitensiometers, J. Hydrol. 188/189, 203–223.

Vandervaere, J.P., Vauclin, M., Elrick, D.E., 2000a. Transient flow from tension infiltrometers. Part 1. The two-parameter equation. Soil Sci. Soc. Am. J., in press.

Vandervaere, J.P., Vauclin, M., Elrick, D.E., 2000b. Transient flow from tension infiltrometers. Part 2. Four methods to determine sorptivity and conductivity, Soil Sci. Soc. Am. J., in press.

van Genuchten, M.Th., Wierenga, P.J., 1976. Mass transfer studies in sorbing porous media. Part 1. Analytical solutions. Soil Sci. Soc. Am. J. 40, 473–480.

Vauclin, M., Chopart, J.L., 1992. L'infiltrométrie multidisques pour la détermination in situ des caractéristiques hydrodynamiques de la surface d'un sol gravillonnaire de Côte-d'Ivoire. L'Agronomie Tropicale. 46, 259–271.

Vauclin, M., Vieira, S.R., Bernard, R., Hatfield, J.L., 1982. Spatial variability of the surface temperature along two transacts of a bare-soil. Water Resour. Res. 18, 1677–1686.

Vauclin, M., Vieira, S.R., Vachaud, G., Nielsen, D.R., 1983. The use of cokriging with limited field soil observations. Soil Sci. Soc. Am. J. 47, 175–184.

Vauclin, M., Elrick, D.E., Thony, J.L., Vachaud, G., Revol, Ph., Ruelle, P., 1994. Hydraulic conductivity measurements of the spatial variability of a loamy soil. Soil Technol. 7, 181–195.

Vogeler, I., Clothier, B.E., Green, S.R., Scotter, D.R., Tillman, R.W., 1996. Characterizing water and solute movement by time domain reflectrometry and disc permeametry. Soil Sci. Soc. Am. J. 60, 5–12.

Wang, D., Yates, S.R., Lowery, B., van Genuchten, M.Th., 1988. Estimating soil hydraulic properties using tension infiltrometers with varying disc permeameters. Soil Sci. 163 (5), 356–361.

Wang, D., Yates, S.R., Ernst, F.F., 1998. Determining soil hydraulic properties using tension infiltrometers, time domain reflectrometry and tensiometers. Soil Sci. Soc. Am. J. 62, 318–325.

Warrick, A.W., 1992. Models for disc permeameters. Water Resour. Res. 28, 1319–1327.

Warrick, A.W., Broadbridge, P., 1992. Sorptivity and macroscopic capillary length relationships. Water Resour. Res. 28, 427–431.

Warrick, A.W., Lomen, D.O., 1976. Time-dependent linearized infiltration. Part III. Strip and disc sources. Soil Sci. Soc. Am. J. 40, 639–643.

Weir, G.J., 1987. Steady infiltration from small shallow circular ponds. Water Resour. Res. 23, 733–736.

White, I., 1987. Comments on "Sorptivity approximations" by Kutilek and Valentova. Transp. Porous Media 2, 317–322.

White, I., Perroux, K.M., 1989. Estimation of unsaturated hydraulic conductivity from field sorptivity measurements. Soil Sci. Soc. Am. J. 53, 324–329.

White, I., Sully, M.J., 1987. Macroscopic and microscopic capillary length and times scales from field infiltration. Water Resour. Res. 23, 1514–1522.

White, I., Sully, M.J., 1992. On the variability and use of the hydraulic conductivity alpha parameter in stochastic treatments of unsaturated flow. Water Resour. Res. 28, 209–213.

White, I., Sully, M.J., Perroux, K.M., 1992. Measurement of surface-soil hydraulic properties: disc permeameters, tension infiltrometers and other techniques. In: Topp, G.C., et al. (Eds.), Advances in Measurement of Soil Physical Properties: Bringing Theory into Practice. Soil Sci. Soc. Am. Spec. Publ. 30. SSSA, Madisson, WI, pp. 69–103.

Wooding, R.A., 1968. Steady infiltration from a shallow circular pond. Water Resour. Res. 4, 1259–1273.

Yeh, T.C., Gelhar, L.W., Gutjahr, A.L., 1985a. Stochastic analysis of unsaturated flow in heterogeneous soils. Part 1. Statistically isotropic media. Water Resour. Res. 21, 447–456.

Yeh, T.C., Gelhar, L.W., Gutjahr, A.L., 1985b. Stochastic analysis of unsaturated flow in heterogeneous soils. Part 2. Statistically anisotropic media with variable α. Water Resour. Res. 21, 457–464.

Yeh, T.C., Gelhar, L.W., Gutjahr, A.L., 1985c. Stochastic analysis of unsaturated flow in heterogeneous soils. Part 3. Observations and applications. Water Resour. Res. 21, 465–471.

Youngs, E.G., Leeds-Harrison, P.B., Elrick, D.E., 1995. The hydraulic conductivity of low permeability wet soils used as landfill lining and capping material: analysis of pressure infiltrometer measurements. Soil Technol. 8, 153–160.

Zhang, R., 1997. Determination of soil sorptivity and hydraulic conductivity from the disc infiltrometer. Soil Sci. Soc. Am. J. 61, 1024–1030.